Assessment of Sustainable Aviation Fuel Production Potential Using Crop Allocation Optimization

by

Yuxin Shu

B.S. Aerospace Engineering, Pennsylvania State University

Submitted to the Department of Aeronautics and Astronautics
in partial fulfillment of the requirements for the degree of

MASTER OF SCIENCE IN AERONAUTICS AND ASTRONAUTICS

at the

MASSACHUSETTS INSTITUTE OF TECHNOLOGY

May 2024

Authored by: Yuxin Shu
Department of Aeronautics and Astronautics
May 14, 2024

Certified by: Ian A. Waitz
Jerome C. Hunsaker Professor of Aeronautics and Astronautics
Vice Chancellor for Undergraduate and Graduate Education
Thesis Supervisor

Certified by: Florian Allroggen
Executive Director, Aerospace Climate Sustainability
Department of Aeronautics and Astronautics
Thesis Supervisor

Accepted by: Jonathan P. How
R.C. Maclaurin Professor of Aeronautics Astronautics
Chair, Graduate Program Committees

Assessment of Sustainable Aviation Fuel Production Potential Using Crop Allocation Optimization

by

Yuxin Shu

Submitted to the Department of Aeronautics and Astronautics
on May 14, 2024 in partial fulfillment of the requirements for the degree of

MASTER OF SCIENCE IN AERONAUTICS AND ASTRONAUTICS

ABSTRACT

Sustainable aviation Fuel (SAF) has been recognized as a viable solution in the near to medium future for decreasing carbon emissions in the aviation industry. Global SAF production, however, is limited and falls well short of the International Air Transport Association's (IATA) goal to achieve net-zero carbon emissions in 2050. This thesis quantifies the global SAF production potential through different crop allocation strategies. Biomass potential is quantified by land suitability and agricultural availability. An optimization model is developed using binary integer linear programming with three crop allocation strategies for 2050 and 2100: fuel maximization, emissions minimization, and land use minimization. The results are shown through six case studies: the United Kingdom, Japan, Australia, Kenya, Brazil, and the United States. Under the Intergovernmental Panel on Climate Change (IPCC) climate scenarios, the globally suitable land can meet and exceed the requirement for biomass cultivation for the aviation sector from the International Energy Agency (IEA). The demand for jet fuel in the U.S. can be fulfilled with 100% SAF, resulting in 21.3% emission savings if optimized for minimum emissions and assuming the use of energy crops. Incorporating lignocellulosic biomass could result in an additional 63.8% reduction in emissions. The study also shows that Japan and the United Kingdom have insufficient agricultural potential to meet their respective domestic SAF demands. In contrast, Australia, Kenya, Brazil, and the United States have agricultural potential that meet or exceed their relative SAF needs.

Thesis supervisor: Ian A. Waitz
Title: Jerome C. Hunsaker Professor of Aeronautics and Astronautics

Thesis supervisor: Florian Allroggen
Title: Executive Director, Aerospace Climate Sustainability

Acknowledgments

I am deeply grateful to a group of remarkable individuals who supported me throughout my journey at MIT. Thank you to my parents for their unwavering support and love. Special appreciation to my advisors, Ian Waitz and Florian Allroggen, for their invaluable guidance and mentorship, which have been crucial in shaping my development as a confident researcher. Thanks also to my friends at MIT for their humor that brightened my days, and to those from Penn State for their warm encouragement. A special thanks to my furry companion, Dewy, who is dedicated to waking me at 6 am daily for his breakfast.

Contents

List of Figures

List of Tables

Chapter 1

Introduction

In 2022, commercial aviation accounted for approximately 2% of global carbon dioxide (CO_2) emissions [25]. The energy-related emissions contributed by aviation will continue to grow as aviation activity is expected to increase by 3.6% annually from 2019-2042 [3]. There are several strategies that have been proposed to achieve carbon neutrality in the aviation industry. Since some of these, like aircraft electrification and new methods of propelling aircraft, are far from being put into practice [38, 41], sustainable aviation fuel (SAF) has been identified as a short to mid-term option for mitigating aviation environmental impact. Compared with petroleum-based conventional jet fuel, SAF has similar chemical and physical characteristics to jet fuel which makes it a drop-in fuel. The life cycle emissions of SAF are lower than traditional jet fuel as SAF uses renewable feedstocks.

According to the International Air Transport Association (IATA), in order to achieve net-zero carbon emissions by 2050, nearly 450 billion liters of sustainable aviation fuel (SAF) will be required each year [21]. However, as of 2023, only slightly more than 600 million liters of SAF are being produced annually, which is less than 0.2% of global jet fuel [22]. Staples et al. have shown that over 50% of the maximum SAF production projected for 2050 can be achieved using biomass crops, including starchy crops, vegetable oil crops, and lignocellulosic energy crops [43]. This highlights the potential of energy crops in scaling up

the production of SAF. Agricultural and forestry residues and wastes can also be used as feedstock, and no additional land is required for these feedstocks. However, these resources are insufficient in expanding SAF production due to their limited potential quantities [9]. Therefore, increasing SAF production is critical, and biomass crops have the potential to make a significant contribution to SAF production expansion.

Several studies have analyzed the potential for SAF production. Ng et al. reviewed the global commercial SAF development from the perspective of technologies, potential feedstock, and policies. They found that hydroprocessed esters and fatty acids (HEFA) is the most commercially developed pathway for SAF production, and more studies are needed for lignocellulosic biomass and waste feedstock [34]. They further recommend SAF-related policies such as reevaluating the blending mandate and multiplier in the Renewable Energy Directive (RED II) to mitigate the negative effects of feedstock competition between the road transport and aviation biofuel sectors. Staples et al. quantified the worldwide potential for SAF production and showed that using SAF can reduce up to 68.1% of lifecycle emissions and offset over 85% of fuel demand for the aviation industry in 2050 [43]. Cantarella et al. determined that sugarcane, eucalyptus, and soybean are the optimal feedstocks for SAF production in Brazil. They estimated that the energy content of sugarcane ethanol produced from 30 Mha of suitable land in Brazil is close to 50% of the energy content of 2015 global aviation kerosene consumption (8.8 EJ per year) [7]. However, no previous study has evaluated the SAF potential using high-resolution geospatial scales with all feasible energy crops and considered Induced Land Use change (ILUC) emissions as part of that analysis.

This study is the first to analyze the global production potential of SAF through crop allocation optimization. In this study, We first evaluate suitable land that could converted for crop cultivation by considering land use restrictions. We estimate the agricultural yields of crops that are eligible for SAF production. The residues and waste are excluded from this study due to the unavailability of sufficient data. Sustainable aviation fuel production is optimized using a binary integer linear programming model under three objectives: Minimize

Emissions (MinE), Minimize Land Use (MinL), and Maximize Fuel Production (MaxF), subject to jet fuel demand and associated life cycle emissions. Results are presented via six country-level case studies: the United Kingdom, Japan, Kenya, Brazil, Australia, and the United States. A comparative analysis assessing the potential of lignocellulosic biomass with miscanthus and switchgrass in fuel production is also included.

Chapter 2

Methods

We begin with identifying the global suitable land that could be converted to cropland for biomass cultivation. Following this, we evaluate the agricultural productivity for 50 crops on suitable land. We select crops for SAF production as informed by land suitability, agricultural yields, and approved feedstock list for SAF production from the Carbon Offsetting and Reduction Scheme for International Aviation framework (CORSIA). We then identify the SAF conversion pathways relevant to each chosen feedstock and calculate SAF conversion factors and lifecycle emissions associated with the SAF pathways. Next, we quantify the jet fuel demand at the country level by aggregating the airport-level jet fuel demand and then calculating the associated emissions threshold. These elements are then fed into the linear optimization model to determine the allocation of feedstock for SAF production in the counties we selected for the case study. The optimization model is designed with two scenarios related to socioeconomic and radiative forcing factors and three strategic objectives: Minimizing Emissions (MinE), Minimizing Land Use (MinL), and Maximizing Fuel Production (MaxF). The summary of this study is outlined in the flowchart in Figure 2.1.

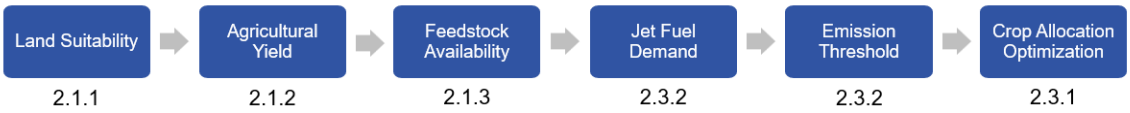

Figure 2.1: Overview of method.

2.1 Biomass Potential

This analysis uses two scenarios, each combining two parameters shown in Table 2.1 to describe the variability of future development. Shared Socio-Economic Pathways (SSPs), one of the parameters, are a set of storylines used in climate change research to describe plausible future socioeconomic developments and their potential impact on greenhouse gas emissions, climate change mitigation and adaptation efforts [37]. There are five narratives: SSP1, SSP2, SSP3, SSP4, and SSP5. The narrative of SSP1 is "Sustainability - Taking the Green Road", which describes a low challenge to mitigation and adoption scenarios, as the world shifts toward a more sustainable direction. SSP2, "Middle of the Road", follows the historical social, economic, and technological path, and it presents a moderate challenge to both mitigation and adaptation efforts. The second parameter is Representative Concentration Pathways (RCPs) which are used in climate science to represent different greenhouse gas concentration trajectories and their potential impacts on future climate change [1]. Four RCPs were presented in the IPCC fifth assessment report with the unit of watts per meter squared: RCP2.6, RCP4.5, RCP6.0, and RCP8.5 [10]. There are various combinations of SSPs and RCPs that can be adopted, with the RCPs ordered by increasing mitigation and the SSPs ordered by increasing mitigation challenges. Table 2.1 shows two scenarios used in this work.

Table 2.1: Scenario assumptions.

	Scenario 1 (S1)	**Scenario 2 (S2)**
Shared Socio-Economic Pathways (SSPs)	SSP1	SSP2
Representative Concentration Pathways (RCPs)	RCP2.6	RCP4.5

2.1.1 Land Suitability

Land suitability is estimated using data from the Land Use Harmonization (LUH2) model developed by the World Climate Research Program coupled Model Intercomparison Project

(CMIP6) [17–19]. LUH2 contains land use projections with a spatial resolution of 0.25 x 0.25 degrees annually across both of the scenarios listed in Table 2.1.

The land categories considered for potential conversion into cropland for SAF production include non-forested primary land, non-forested secondary land, and pastureland. Primary land is characterized as terrain that has remained undisturbed by human actions since 1700 AD. Secondary land refers to terrain that has experienced human disturbance post-1700 AD and is currently undergoing natural restoration. Forested primary and secondary land were not considered as suitable land in this study in order to protect biodiversity, and cropland was excluded to avoid competition with food production. All protected areas, as identified by the World Database on Protected Areas (WDPA) from Protected Planet, are considered unavailable for conversion to crop cultivation [44]. WDPA is a joint project between the UN Environment Programme and the International Union for Conservation of Nature (IUCN), which contains both terrestrial and inland waters protected areas.

To limit competition for livestock grazing and fulfill meat demand, the pastureland availability is estimated using data sets from the SSP Database version 2, which was developed by the International Institute for Applied Systems Analysis (IIASA) and the National Center for Atmospheric Research (NCAR) [35]. The SSP Database contains population projections every ten years for both scenarios. In Scenario 1 (S1), which combines SSP1 and RCP2.6, we assume that per capita meat consumption adheres to the Healthy Diet (HDiet) guidelines from Harvard Medical School, with consumption levels remaining constant throughout. In contrast, Scenario 2 (S2) anticipates an approximately 30% increase in livestock demand compared to S1 [27], and, accordingly, we project the same 30% rise in meat consumption in S2 compared to S1. Additionally, we assume the meat per livestock data from Our World in Data [36] and land intensity of livestock per acre remain unchanged. The resulting pastureland availability under S1 is 65 % for 2050 and 67 % for 2100. For S2, pastureland availability is 60 % and 57 % for 2050 and 2100 respectively. All pastureland availability from 2030 to 2100 for each decade is shown in Table B.1.

2.1.2 Agricultural Yield

The agricultural yield is estimated using data from the Global Agro-ecological Zones (GAEZ) version 4.0 model, which is developed by the Food and Agriculture Organization of United Nations (FAO) and the International Institute of Applied System Analysis (IIASA) [12]. The GAEZ model projects the attainable yield of 50 crops on a 5-arc-minute grid cell resolution for Scenario 1 and Scenario 2 considering 6 different climate models by evaluating crop-specific growth requirements aligned with local climate and soil conditions across different agricultural input levels and time frames. The attainable yield is presented in increments of 30 years. Three specific 30-year periods: 2011-2040, 2041-2070, and 2071-2100 are selected for the analysis. Also, land suitability is further limited by using the GAEZ model. Based on the suitability index (SI) from the GAEZ model, any land with a suitability level below "moderate" (SI = 2500) is excluded from consideration to avoid land where crops are unlikely to be cultivated. In this analysis, we assume the GFDL-ESM2M climate model, high input levels, no CO2 fertilization, and rain-fed systems to mitigate the diversion of water resources from food crops or human consumption.

2.1.3 Feedstock Availability

To calculate the availability of feedstocks for SAF, the land suitability is interpolated into agricultural yield at the relatively higher resolution grid scale of 5-arc-minute. The data set after interpolation provides the agricultural yield of feedstocks by land type in each grid cell, which is utilized for the feedstock availability calculation and as inputs to the SAF production optimization.

2.2 Projection of SAF Production

2.2.1 Feedstock Selection

Twelve energy crops are selected as potential SAF feedstocks according to the GAEZ model and CORSIA-certified crops: maize, sugarcane, sorghum, wheat, miscanthus, switchgrass, soybean, rapeseed, sunflower, jatropha, oil palm, and sugarbeet. The baseline feedstock assumption excludes miscanthus and switchgrass; these are included in a separate scenario. Because of the physical barriers created by lignin, commercial production of SAF through lignocellulosic biomass is still under development [28]. Additionally, according to the American Society for Testing and Materials (ASTM) D7566 Annex A3 [4], the maximum blend ratio of the Synthesized Iso-Paraffins (SIP) pathway with sugarbeet as feedstock is 10 %. If the portion of SAF production from the sugarbeet exceeds 10 %, the sugarbeet is also removed from the baseline feedstock assumptions. Moreover, because of the uniqueness of feedstock availability in each country, the selection of crops will be different, but it will remain within the scope of the crops listed previously. If the suitable yield of feedstock is zero in feedstock availability, it will not count as feedstock for further optimization. This analysis focuses only on energy crops, thereby excluding all residues, waste fats, oils, and greases (FOGs), and municipal solid waste (MSW). Furthermore, the practice of double cropping is not accounted for in this study.

2.2.2 Feedstock to Fuel Conversion

In this analysis, four CORSIA-qualified SAF pathways associated with crops are considered: Alcohol-to-Jet (ATJ), Hydroprocessed Esters and Fatty Acids (HEFA), Fischer Tropsch (FT), and Synthesized Iso-Paraffins (SIP) [24]. The conversion pathways corresponding to each crop are shown in Table 2.2, and only a single pathway is selected for each feedstock.

Table 2.2: Crops considered as feedstocks and corresponding pathways. [24]

Crop	**Type**	**Pathway**
Maize	C4 annual	ATJ
Sugarcane	C4 annual	
Sorghum	C4 annual	
Wheat	C3 annual	
Soybean	C3 nitrogen-fixing	HEFA
Rapeseed	C3 annual	
Sunflower	C3 annual	
Jatropha	C3 perennial	
Oil Palm	C3 perennial	
Miscanthus	C4 perennial	FT
Switchgrass	C4 perennial	
Sugarbeet	C3 annual	SIP

SAF production for the ATJ pathway is calculated by.

$$SAF\left[\frac{MJ}{ha}\right] = y_G\left[\frac{kg_G}{ha}\right] \cdot f_{GtI}\left[\frac{kg_{WW}}{kg_G}\right] \cdot f_{ItE}\left[\frac{MJ_{EtOH}}{kg_{WW}}\right] \cdot f_{EtJ}\left[\frac{MJ_{Jet}}{MJ_{EtOH}}\right] \tag{2.1}$$

In Equation 2.1, y_G is the crop yield from the GAEZ Model, and different crops have different GAEZ units such as kg Sugar per ha and kg Dry Weight per ha. f_{GtI} is the factor to convert one-kilogram GAEZ unit yield to kg Wet Weight intermediate yield, f_{ItE} is the factor to convert intermediate yield to MJ of Ethanol, and f_{EtJ} is the factor to convert MJ of Ethanol to MJ of SAF since the process produces additional energy carriers such as diesel, naphtha, and heavy oil. Factors shown in Table A.1 used for each crop are based on the GREET (Greenhouse gases, Regulated Emissions, and Energy use in Technologies) Model [5], and Demsky's work [11].

SAF production for the HEFA pathway is modeled as follows.

$$SAF\left[\frac{MJ}{ha}\right] = y_G\left[\frac{kg_G}{ha}\right] \cdot f_{GtO}\left[\frac{kg_{Oil}}{kg_G}\right] \cdot f_{OtJ}\left[\frac{MJ_{Jet}}{kg_{Oil}}\right] \tag{2.2}$$

In Equation 2.2, y_G is the crop yield in GAEZ unit kg Dry Weight per ha or kg Oil per ha. f_{GtO} is the factor used to convert kg GAEZ unit to feedstock in kg oil and f_{OtJ} is the

factor to convert oil to MJ of SAF. The co-products include light gases, naphtha, and diesel. The factors are from the GREET Model and the CORSIA document and are listed in Table A.3.

SAF production for the FT pathway shown in Equation 2.3 is similar to the HEFA pathway. The factors in Tabel A.2 are calculated from the GREET model and Zang's work [48].

$$SAF\left[\frac{MJ}{ha}\right] = y_G\left[\frac{kg_G}{ha}\right] \cdot f_{GtI}\left[\frac{kg_{DW}}{kg_G}\right] \cdot f_{ItJ}\left[\frac{MJ_{Jet}}{kg_{DW}}\right] \tag{2.3}$$

SAF production for the SIP pathway is formulated below:

$$SAF\left[\frac{MJ}{ha}\right] = y_G\left[\frac{kg_G}{ha}\right] \cdot f_{GtI}\left[\frac{kg_{DW}}{kg_G}\right] \cdot f_{ItJ}\left[\frac{MJ_{Jet}}{kg_{DW}}\right] \tag{2.4}$$

In Equation 2.4, the unit of y_G is kg Sugar per ha. f_{GtI} is the factor that converts kg GAEZ unit to kg Dry Weight, and f_{ItJ} is used to convert intermediate yield in kg Dry Weight to SAF in MJ. Unlike other pathways, there are no co-products for the SIP pathway. Factors are from Gruska [15] and Kelso's work [20], listed in Table A.4.

2.2.3 Life Cycle Assessment of SAF

To quantify the emission from SAF production from different crops, the analysis of lifecycle greenhouse gases (GHG) emissions is used to assess the potential environmental impact of the entire production process. The LCA factor is the summation of core life cycle emission and Induced Land Use Change (ILUC) emission values with the unit of gCO_2e/MJ_{SAF}. Induced land use change emissions are defined as emissions generated from additional land use change, including both direct and indirect land use change. Direct land use change happens in areas where new SAF is produced, and indirect land use change is in the places due to the displacement of crops or animals occupying the land previously. All factors are from the CORSIA documentation [24] and are listed in Table A.6.

2.3 Optimization

2.3.1 Objective Functions

The technique used for mathematical modeling is Linear Programming (LP), which optimizes a linear objective function subject to linear constraints. It uses the simplex algorithm to navigate feasible solutions and find the optimum. The optimization model is developed in Python version 3.9.15 with PuLP version 2.7.0 and solved by the Gurobi Optimizer version 10.0.3 with 2 % relative gap tolerance.

The first of three optimization cases is to minimize the total emission in the chosen country while meeting fuel demand if possible. The total emission function in Eqn.2.5 calculates the total emission by summing up the emissions for each crop i in each cell c.

$$\text{Minimize} \quad E = \sum_{c=1}^{N} \sum_{i=1}^{M} e_{c,i} \cdot x_{c,i} \tag{2.5}$$

Table 2.3: Parameters in optimization model.

Symbol	Description
$e_{c,i}$	CO_2 emissions associated with selecting crop i in cell c
$f_{c,i}$	Fuel production associated with selecting crop i in cell c
N	Number of cells
M	Number of crop types
$F_{\text{threshold}}$	Fuel demand for country
$E_{\text{threshold}}$	Emission requirement

The variable $x_{c,i}$ is a binary decision variable where:

$$x_{c,i} = \begin{cases} 1 & \text{if crop } i \text{ is selected for cell } c \\ 0 & \text{otherwise} \end{cases} \tag{2.6}$$

The crop selection constraint equation is defined in Eqn 2.7.

$$\sum_{i=1}^{M} x_{c,i} = 1, \quad \forall c \in \{1, \ldots, N\} \tag{2.7}$$

To ensure the total fuel produced by selected crops reaches the country's fuel demand, one constraint is defined for fuel production in Eqn 2.8.

$$\sum_{c=1}^{N} \sum_{i=1}^{M} f_{c,i} \cdot x_{c,i} \geq F_{\text{threshold}} \tag{2.8}$$

To further limit the range of emission, the constraint of emission is used to ensure the result is below the emission requirement shown in Eqn 2.9.

$$\sum_{c=1}^{N} \sum_{i=1}^{M} e_{c,i} \cdot x_{c,i} \leq E_{\text{threshold}} \tag{2.9}$$

The second of three optimization cases is to minimize the total land used to produce SAF in a specific country while meeting fuel demand if possible. The objective function is formulated as follows:

$$\text{Minimize} \quad L = \sum_{c=1}^{N} \sum_{i=1}^{M} l_{c,i} \cdot x_{c,i} \tag{2.10}$$

$l_{c,i}$: Land area used associated with selecting crop i in cell c

The variable is the same binary decision variable in Eq 2.6 and all three constraints in Eqn 2.7-2.9 are used in minimizing land area objective as well.

The last of the three optimization cases is to maximize the fuel production while not exceeding the Jet-A emissions level. Compared to the other two objectives, the only difference is the objective function in Eqn 2.11. The linear programming objective changes from Minimize to Maximize, and the three constraints remain the same.

$$\text{Maximize} \quad F = \sum_{c=1}^{N} \sum_{i=1}^{M} l_{f,i} \cdot x_{c,i} \tag{2.11}$$

2.3.2 Thresholds in Constraints

In this analysis, the anticipated demand for jet fuel consumed for airports within each country is estimated to be the same across both scenarios. The projection leverages commercial passenger flight schedules from the year 2019, sourced from OAG data. To accurately estimate fuel consumption for an aircraft operating on a route, we employ the Aviation Emissions Inventory Code (AEIC) and apply it to each specified pairing of aircraft and route. A linear fit shown in Eqn 2.12 derived for the worldwide total commercial airlines fuel consumption between 2005 and 2019 is used to extrapolate the fuel demand to 2100 [23]. Data in 2020 and 2021 are excluded because of the pandemic.

$$\text{Global Jet Fuel Demand [Billion Gallons]} = 1.9821 \cdot year - 3911.1 \tag{2.12}$$

The projected country-level jet fuel demand is calculated by multiplying the country-level jet fuel demand in 2019 with the global fuel increase ratio from Eqn 2.13.

$$\text{Jet Fuel Demand} = 2019\ Jet\ Fuel\ Consumption_{(country)} \cdot \frac{IATA(year)}{IATA\ 2019} \tag{2.13}$$

The emission requirement in Eqn.2.14 is the multiplication of the LCA emission of petroleum jet fuel and the jet fuel demand. The coefficient 89 gCO_2/MJ is the LCA of petroleum jet fuel [24].

$$\text{Emission Requirement}\,[gCO_2e] = 89 \left[\frac{gCO_2e}{MJ_{fuel}}\right] \cdot Jet\ Fuel\ Demand\,[MJ] \tag{2.14}$$

Chapter 3

Results

3.1 Land Potential for SAF Production

Our assessment begins with estimating the suitable land for biomass production in 2050 and 2100 under two distinct scenarios: Scenario 1(S1) and Scenario 2 (S2). We assume that all non-forested primary and secondary land and available pastureland are considered for conversion to cropland. Land areas belonging to these three land types with a Suitability Index (SI) above the moderate threshold are considered suitable, and pastureland is further limited by pastureland availability as discussed in Section 2.1.1. Grid cells categorized as protected areas are excluded from land conversion [44]. For cropland, urban, and primary forests, where these categories exceed 50 % of a given grid cell are marked as inappropriate for cropland conversion.

The projected land potential for SAF production under both scenarios and respective years is shown in Table 3.1. Given the global land required for bioenergy cultivation to achieve net-zero emission is estimated at 410 million hectares (Mha) by the year 2050, with 7% allocated to the aviation sector, it is feasible to meet and exceed the area requirement of biomass cultivation for SAF production based on the assumptions made in this study [21]. This emphasizes the substantial opportunity to enhance fuel production through land use.

Table 3.1: Land potential of biomass cultivation for SAF production.

Scenario	Year	Land Potential for SAF Production [Mha]
S1	2050	2332
	2100	2265
S2	2050	2141
	2100	2000

Figure 3.1 presents the map of land potential by category for biomass under Scenario 2 for the year 2050 depicted using the Miller projection. Here the dark blue represents the available non-forested primary and secondary land and available pastureland with a suitability index of $\geq 50\%$ which are considered for conversion to cropland in the optimization cases presented later in this chapter. For additional maps of land potential, refer to Figure B.1.

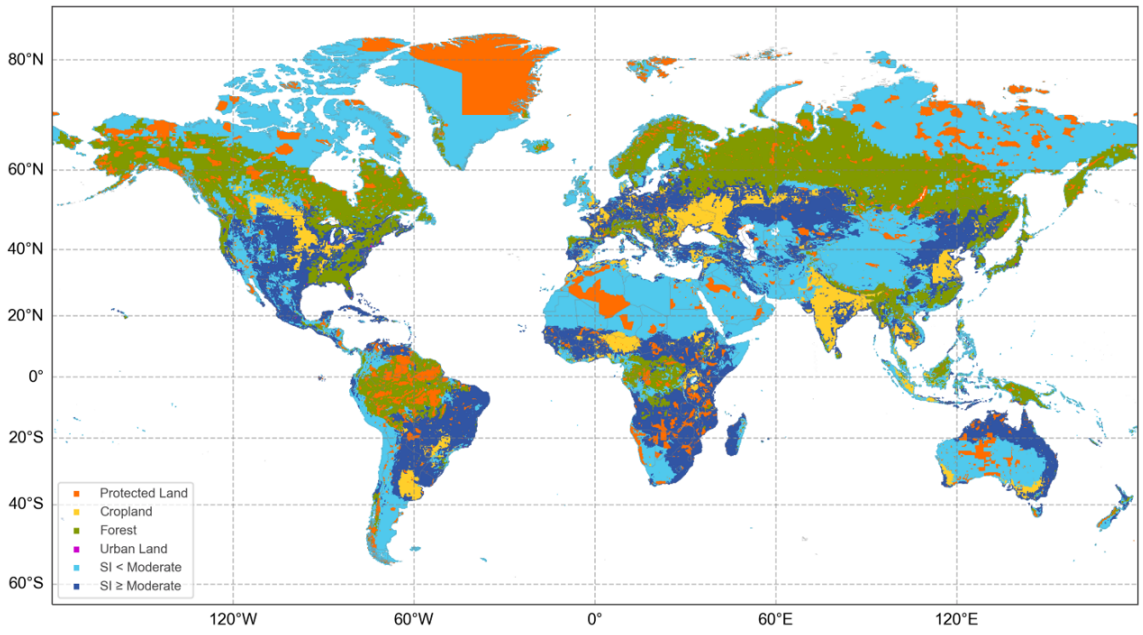

Figure 3.1: Land use by category under Scenario 2 (S2) in 2050 under Miller projection.

3.2 Optimization Results for the United States

In this section, we illustrate the outcomes from the model by utilizing a case study focused on the United States. Full results of the United States and other countries are in Appendix B.

3.2.1 Biomass Potential

Figure 3.2 shows the projected agricultural yields of crops within the Global Agro-Ecological Zones (GAEZ) model for the year 2050 under Scenario 1 (S1) in the United States. Each bar represents the maximum achievable yield for each crop, assuming all suitable land is used exclusively for cultivation. The grey bars show the crops suitable to grow in the U.S. but which have not been assessed by CORSIA for SAF production; the bars in blue present the crops that are not only eligible for biofuel production but are also currently cultivated within the country based on data from the United States Department of Agriculture (USDA) [46]; the orange bars represent the feedstocks which are suitable but have not been planted. According to the analysis, all 12 energy crops detailed in Table 2.2 as SAF production feedstocks are suitable for growth in the U.S., but only 6 of these crops are currently cultivated according to USDA records. The exact yield values of the twelve energy crops in Figure 3.2 are shown in Table B.2.

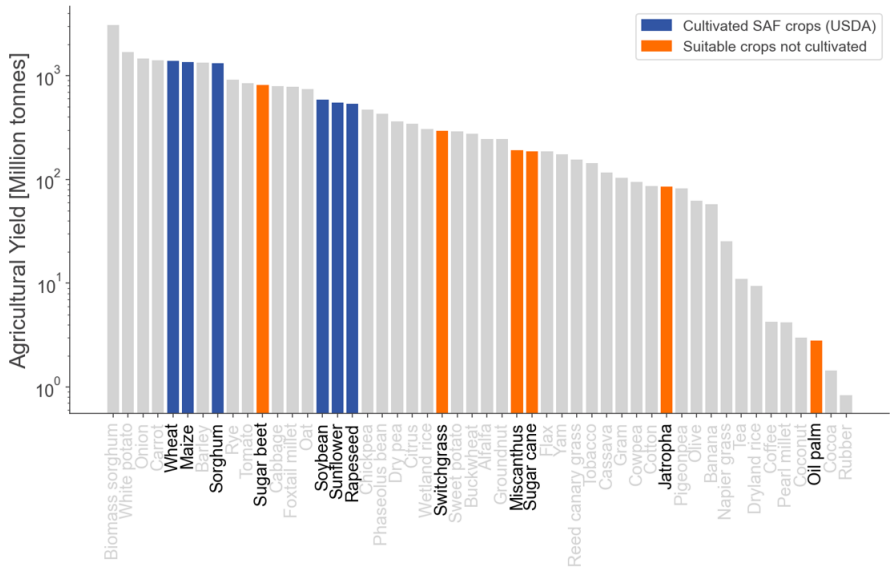

Figure 3.2: Projected agricultural yields of crops under S1 for 2050 in the United States.

Furthermore, Figure 3.3 presents the yield comparison between the present cultivated crop yield and yield which could be realized using the projected suitable land from land expansion in 2050. The projected yield is significantly higher than the current yield from

cropland. The results emphasize the substantial opportunity to scale up the SAF production from energy crops. The projected agricultural yields of selected crops for other scenarios can be found in Table B.2.

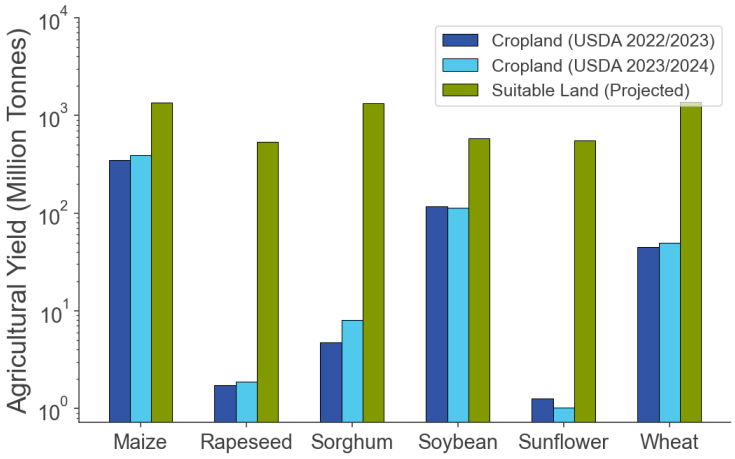

Figure 3.3: Crop yield on projected suitable land in 2050 under S1, compared with the yields in cropland in 2022/2023 and 2023/2024 from USDA in the United States. The crop yields are calculated from all suitable land individually and are not cumulative.

3.2.2 Baseline SAF Potential Projection

The SAF production results across the three optimization objectives for Scenario 1 (S1) and Scenario 2 (S2) in both 2050 and 2100 are shown in Figure 3.4. The baseline feedstock assumption includes maize, sugarcane, sorghum, wheat, soybean, rapeseed, sunflower, jatropha, and oil palm since SAF production from sugarbeet is over the 10 % threshold as discussed in Section 2.2.1. The navy blue bar shows the Minimizing Emission (MinE) results, and the light blue bar represents the Minimizing Land Use (MinL) objective. Both of them are optimized to meet the projected U.S. jet fuel demand. The green bar shows the results of Maximizing the Fuel production (MaxF) objective. Additionally, the dotted line in black is the projected U.S. jet fuel demand for the given year, the red dotted line shows the corresponding emission threshold, and the blue one is the suitable land area threshold.

Based on Section 2.3.2, the projected fuel demand is estimated at 31.8 billion gallons in 2050 with the associated emission threshold at 380.2 million tonnes CO_2e and 52.5 billion

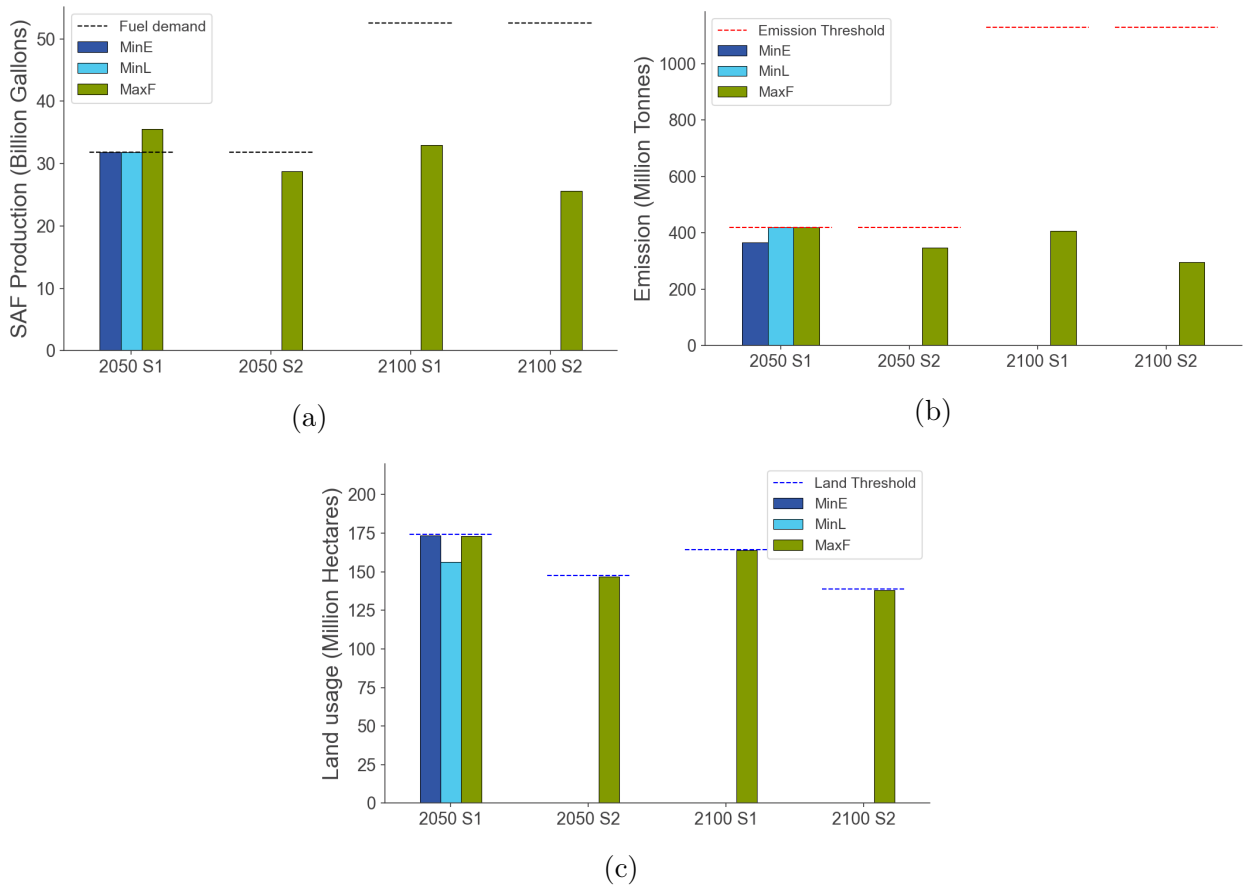

Figure 3.4: (a) SAF production potential, (b) corresponding emission, and (c) land usage for 2050 and 2100 in the United States. MinE, MinL, and MaxF are optimization objectives described in Section 2.3.

gallons with 627.8 million tonnes CO_2e in 2100. Figure 3.4 shows that it is feasible to meet the U.S. jet fuel demand without exceeding the emission threshold associated with the equivalent petroleum jet fuel in 2050 S1 under the assumptions considered in this analysis. It is not possible to meet the jet fuel demand in 2100 under any of the scenarios. The fraction of jet fuel demand met in 2100 S1, 2050 S2, and S2 2100 is 90.6%, 62.7%, and 48.8% respectively, which is limited by the total suitable land area. Scenario 1 generally produces more SAF compared with Scenario 2 due to more land being available and an average 6% higher pastureland availability assumption. The emissions would be 21.3% lower compared to petroleum jet fuel by optimizing for MinE, there is no emission saving for MinL and MaxF, and the maximum fuel production is 11.7% more than the U.S. jet fuel demand in S1

2050. Additionally, in Figure 3.4c, considering the U.S. land area is 914.8 Mha as reported by the Census Bureau [45] and the USGS [47], the proportion of the land area used for MinL to meet SAF demand is 74.2% of suitable land in S1 2050 and 14.1% of the domestic land area. More details of SAF production and emission are in Table B.3.

Figure 3.5 shows the breakdown of the SAF production by crops for Scenario 1 in 2050 under the three optimization objectives. Since the projected SAF production is 11.7% more

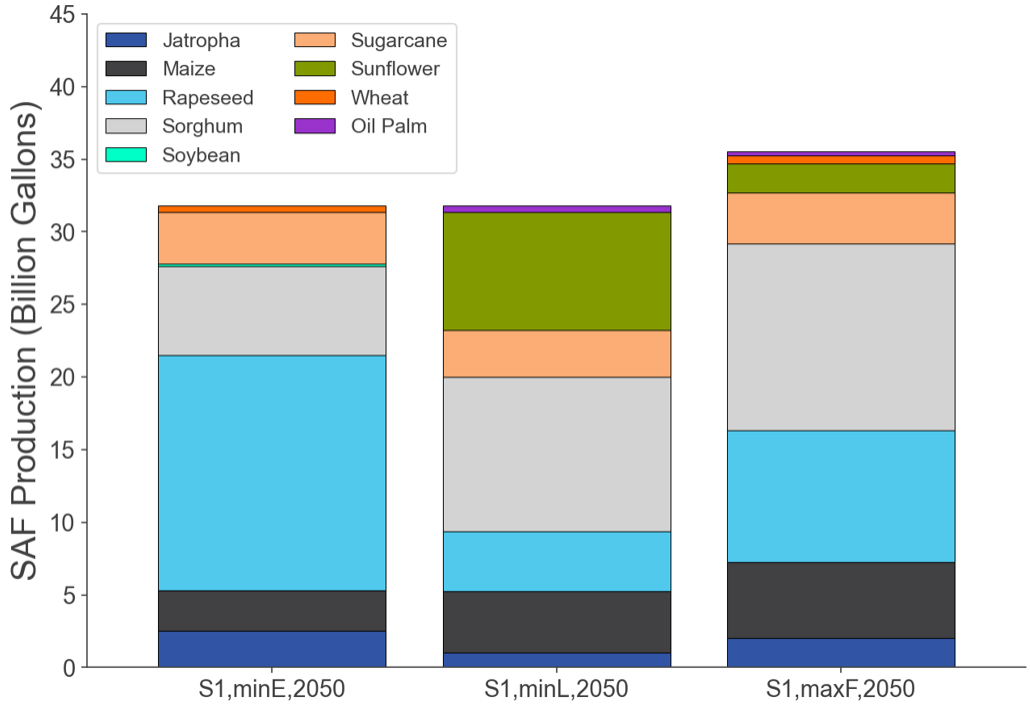

Figure 3.5: SAF production by crop optimized for all objectives under S1 2050 in the United States.

than the demand while optimizing for maximum fuel production, the feedstock selection is skewed to crops with high fuel production efficiency(MJ SAF/ha). For MaxF, 63.9% oil palm yields with the first highest fuel production efficiency are used, but it accounts for 0.77 % of total SAF production because it has the second lowest yields. This situation also makes sugarcane and jatropha, the second and third highest fuel production efficiency crops, not contribute a lot to SAF production. Since the fuel production efficiency of soybean and wheat is much lower than other crops, the SAF production is predominantly in sunflower, maize,

rapeseed, and sorghum. Among them, sorghum contributes to the most SAF production due to its high agricultural yields and relatively low emission intensity (tCO_2 per hectare). The relatively higher emission intensity of maize causes lower production compared with sorghum. Feedstock choices optimized for minimizing land use align closely with those for maximizing fuel production. However, when minimizing emissions, lower-emission rapeseed often replaces the sunflower. Figure 3.6 shows the locations of crops to meet the jet fuel demand for S1 2050 under three objectives. For all objectives, most crops are planted in the West and Midwest. As shown in Figure 3.6, sorghum is planted in the West, and maize is mainly cultivated in Iowa and Missouri. This pattern is present in all objectives to meet the jet fuel demand. The exact values of this plot can be found in Table B.4

To determine the impact of the SIP pathway for optimization, an additional analysis including sugarbeet is conducted, illustrated in Figure 3.7. The detailed value for Figure 3.7 can be found in Table B.5. By comparing with Figure 3.4 which is optimized without sugarbeet, the maximum SAF production in S1 2050 increases by 38.4%, and the emissions are reduced by 42.4%, and 47.1% for MinE and MinL respectively. For MinL, 40.6% of suitable land is utilized to meet the fuel demand, which is 7.7% of U.S. territory. This is expected since sugarbeet has a similar SAF production efficiency (MJ/ha) to sugarcane, which has the second highest SAF production efficiency among the feedstocks used in this study, and the emission intensity is lower than sorghum. In addition, sugarbeet can contribute to a large portion of total SAF production because of its high agricultural yield in the United States. Additionally, it is feasible to optimize the SAF production to meet the jet fuel demand for Scenario 2 in 2050 which has more restricted land area compared with Scenario 1 in 2050. With sugarbeet replacing sorghum and rapeseed as the predominant SAF crop, the high production efficiency of sugarbeet makes it possible to produce more fuel on less land, thus alleviating the effects of land restrictions on SAF production. More results optimized with sugarbeet are in Appendix B.

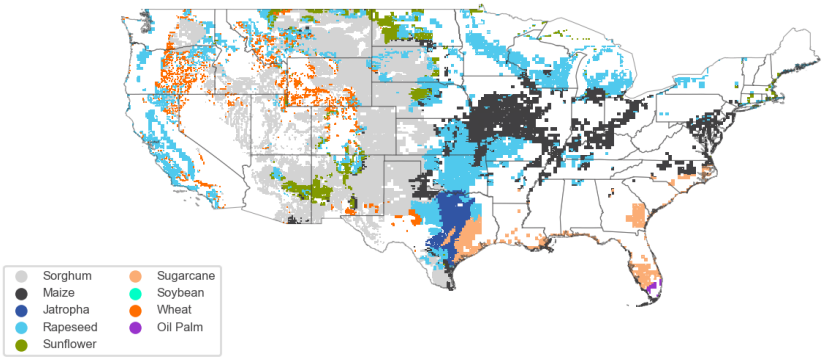

(a) MaxF

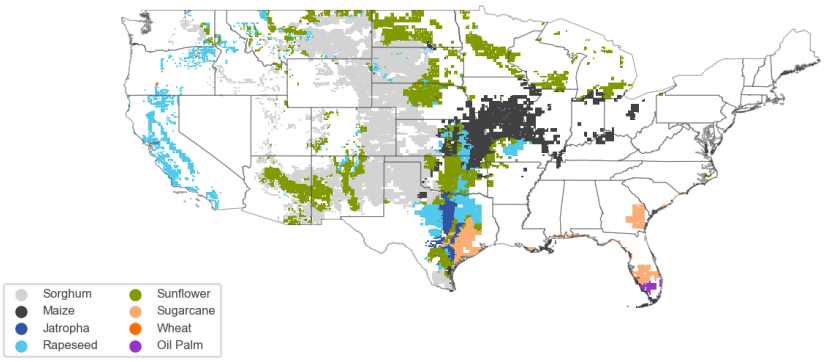

(b) MinL

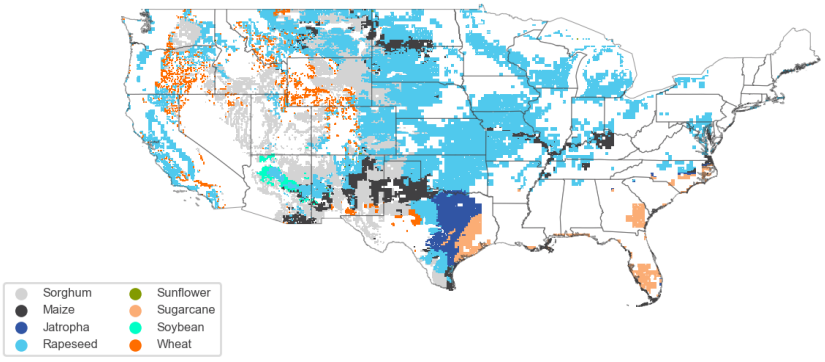

(c) MinE

Figure 3.6: SAF production potential optimized for MaxF (a), MinL (b), and MinE (c) under S1 2050.

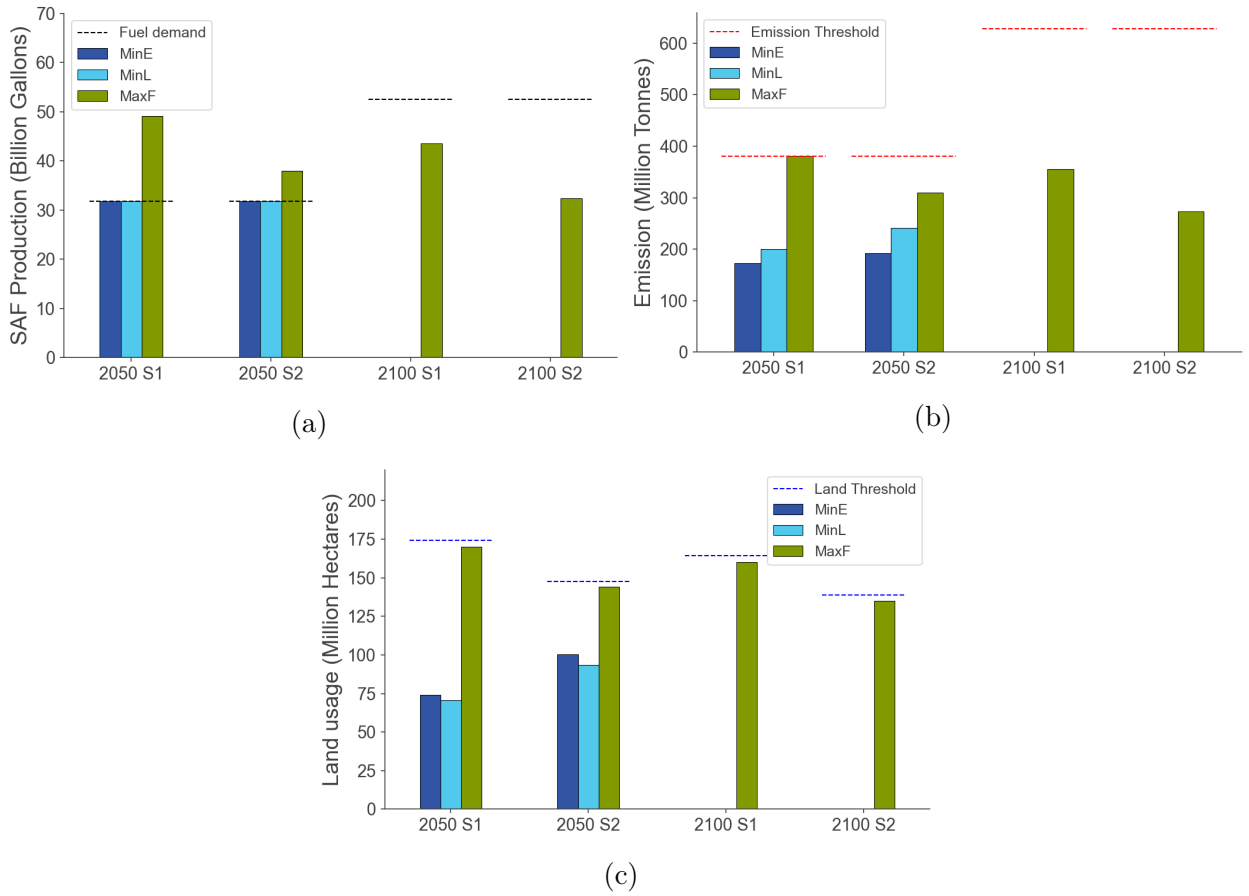

Figure 3.7: (a) SAF production potential, (b) corresponding emission, and (c) land usage with sugarbeet under three objectives for 2050 and 2100 in the United States.

3.3 SAF Potential Case Studies for Different Countries

We show the case studies of countries with different SAF potential, which include Japan, the United Kingdom, Australia, Kenya, Brazil, and the United States from Section 3.2. We classify these countries based on Equation 3.1 which evaluates the viability of SAF production within a given region. It does this by comparing SAF production to jet fuel demand and then adjusting for how effectively the land used for SAF production utilizes the total suitable land. The linearized SAF potential relative to domestic demand is computed specifically for the baseline objective of Maximizing SAF Production (MaxF) across four scenario-year pairings. This is due to the lack of sensitivity in the objective functions for countries that cannot meet their SAF requirements. Suppose the linearized SAF potential

relative to domestic demand is less than 100% for all scenario-year pairs. In that case, the country cannot meet the jet fuel demand and is classified as having a production deficit. The country is categorized as having a production surplus if the production is larger than or equal to 100%. The four scenario-year pairs are S1 2050, S2 2050, S1 2100, and S2 2100.

$$\text{Linearized SAF potential relative to domestic demand (\%)} = \left(\left(\frac{\text{SAF Production}}{\text{Jet Fuel Demand}}\right) / \left(\frac{\text{Used Land}}{\text{Total Suitable Land}}\right)\right) \times 100\% \quad (3.1)$$

Figure 3.8 shows the linearized SAF potential relative to domestic demand for six countries for four scenario-year pairs with the MaxF objective. The SAF potential of Japan and the United Kingdom is less than 100% for any scenario-year pair. They are classified as having the SAF production deficit. This is as expected since these two counties have extremely limited land for SAF production, and the ratio of used land and total suitable land is 1. In contrast, a surplus of SAF can be produced for some other countries where the SAF potential is estimated to be over 100% for at least one scenario-year pair. This emphasizes the heterogeneity of SAF potential across the world and the potential of some countries to scale up SAF production in excess of their country's demand. For countries where the linearized SAF potential relative to demand exceeds 100%, the results demonstrate variability in response to the objective function, as detailed in the Appendix B-G.

3.4 Land Conversion for SAF Production

The types of land that are converted for SAF production to meet jet fuel demand are shown for the different countries and scenarios. As discussed in Section 2.1.1, the land types chosen to convert to cropland are non-forested primary and secondary, and pasture land. In Figure 3.9, the left plot shows the baseline SAF production by land type, and the right side is the land usage by land type for S1 2050 in the United States, related to the results

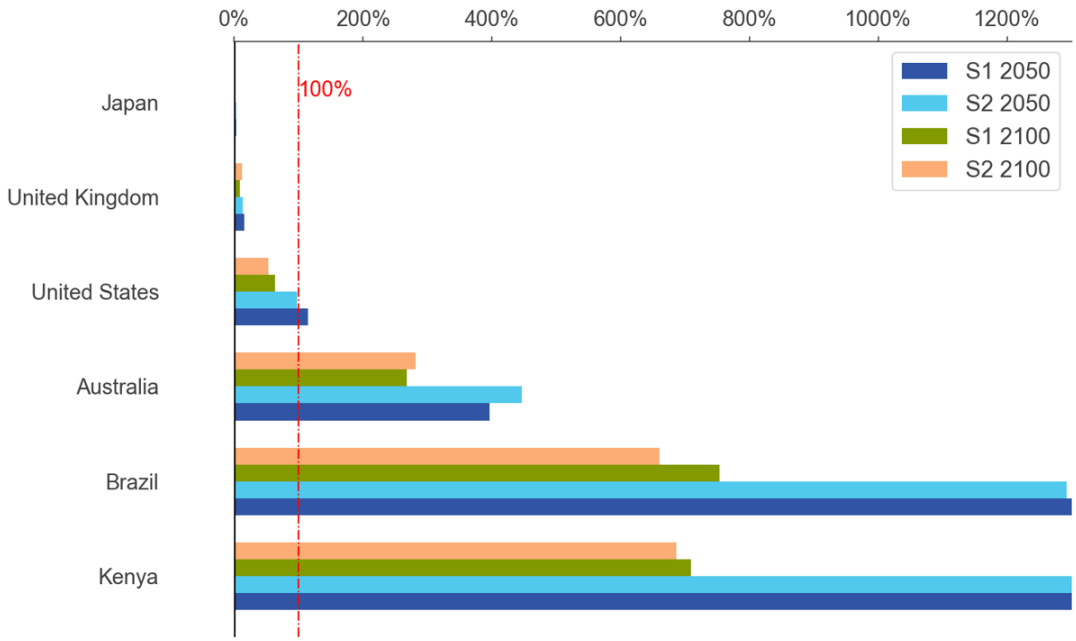

Figure 3.8: Linearized SAF potential relative to domestic demand of six countries four scenario-year pairs under MaxF.

presented in Section 3.2. In the United States, SAF production is mainly from the feedstocks grown on cropland converted from pastureland. To meet the jet fuel demand in the United States through SAF, production will be concentrated in regions with the most suitable land, ensuring the highest yields in those areas. Therefore, the land conversion depends on the amount of each land type for the country in which SAF production is limited by suitable land area. The exact values of Figure 3.9 are shown in Table B.7.

However, the land conversion varies for countries constrained by the emissions threshold since those have more viable land use strategies. Figure 3.10 shows baseline SAF production and land usage by land type under S1 2050 in Kenya. The projected SAF production is limited by the emission threshold in Kenya. For MinL, the predominant land type converted for SAF production is non-forested secondary land since non-forested secondary land has the highest fuel production efficiency (SAF MJ/ha). For MinE and MaxF, the majority of SAF production is almost equally from non-forested secondary and pastureland since the emission intensity (tCO_2/ha) of pastureland is lower than the emission intensity of non-forested

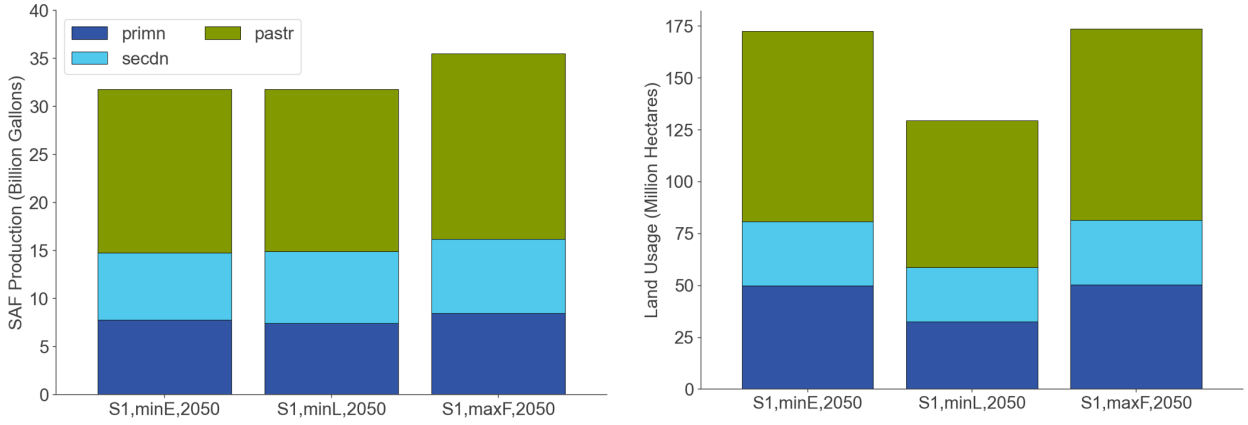

Figure 3.9: Baseline SAF production by land type (left), land usage by land type (right) for all objectives under S1 2050 in the United States.

secondary. Moreover, while non-forested primary land has the lowest emission intensity, its low fuel production efficiency makes it sub-optimal for conversion. The values can be found in Table B.8.

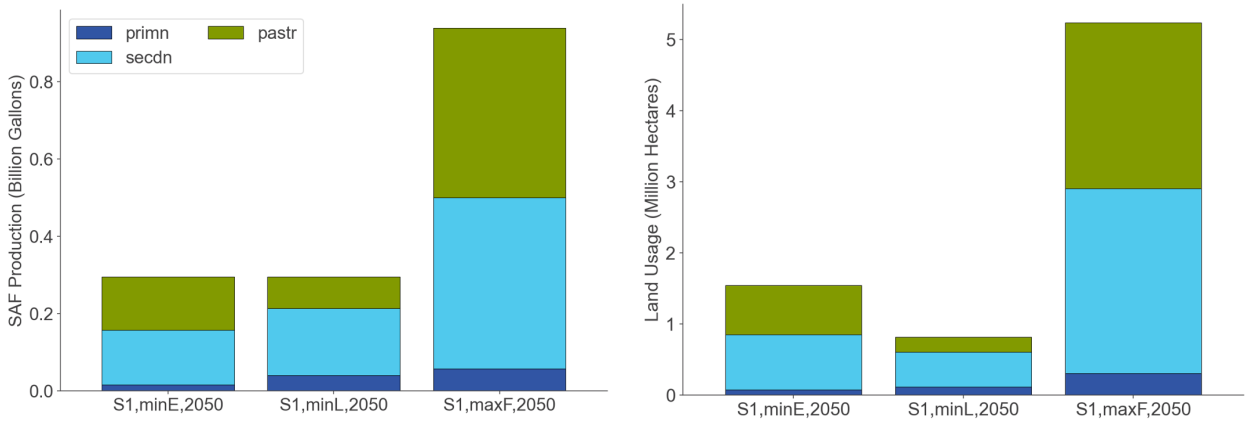

Figure 3.10: Baseline SAF production by land type (left), land usage by land type (right) for all objectives under S1 2050 in Kenya.

3.5 Analysis Considering Lignocellulosic Biomass

This section shows the analysis of the potential of lignocellulosic biomass for SAF production if the technological barrier caused by lignin can be overcome. The two lignocellulosic biomass focusing in this analysis are switchgrass and miscanthus. Figure 3.11 shows the

optimization results with miscanthus and switchgrass in the United States. Compared with baseline SAF production in the U.S. in Figure 3.4 in Section 3.2, more SAF is produced with less carbon emission when lignocellulosic biomass is available as a feedstock. The fuel

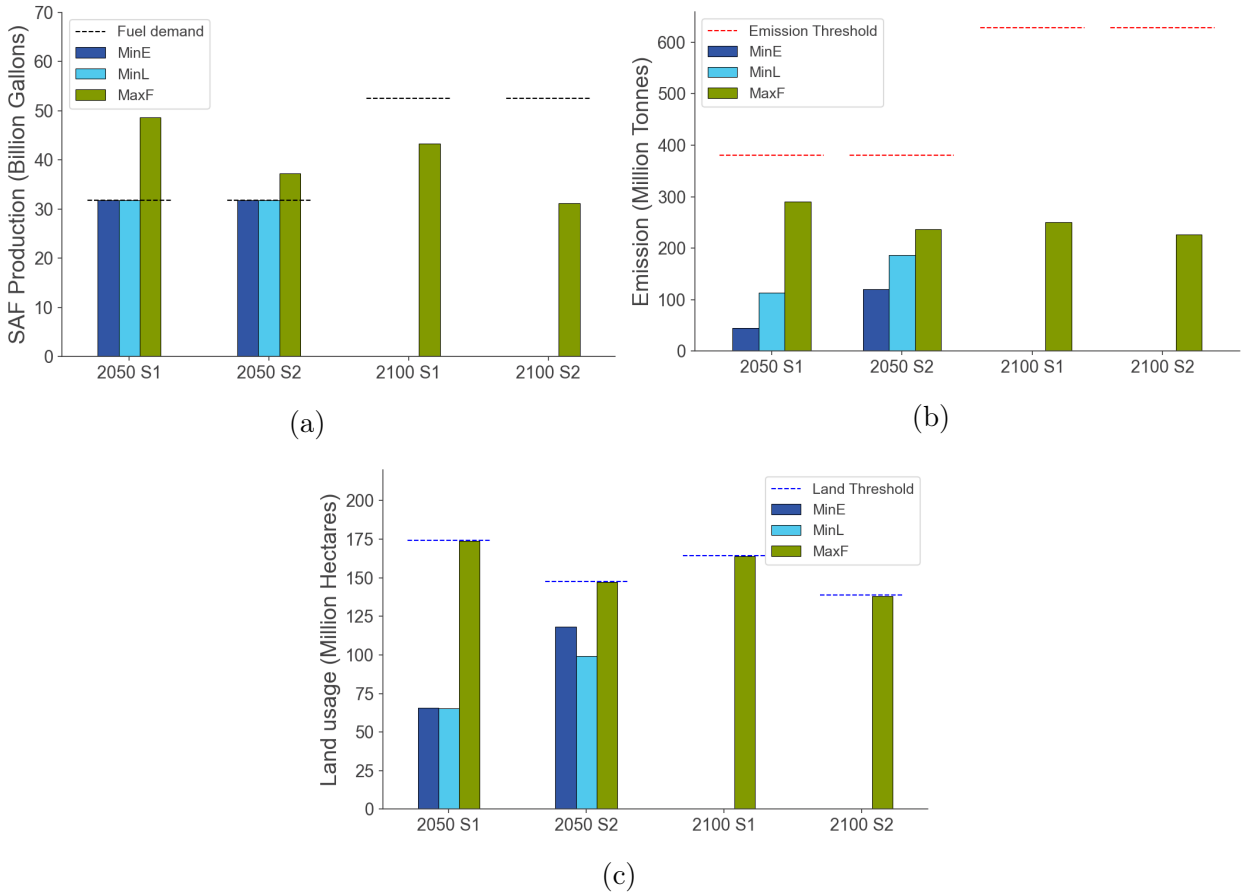

Figure 3.11: SAF production potential (a), corresponding emission (b) and land usage (c) with miscanthus and switchgrass under three objectives for 2050 and 2100 in the United States.

production efficiency of switchgrass and miscanthus is close to sugarcane which has the second highest fuel production efficiency in the baseline scenario. Additionally, the LCA values of switchgrass and miscanthus are 15.7 and -2.2 gCO_2e/MJ respectively, which make them have the lowest and second lowest emission intensity among all feedstock considered in this analysis. Moreover, the high adaptability across diverse geographic regions also enhances the viability of miscanthus and switchgrass as feedstock for SAF production. Even though the projected SAF production with switchgrass and miscanthus is similar to the SAF pro-

duction with sugarbeet in Figure 3.7a, the association emission is an average of 50 % lower than emission with sugarbeet.

Chapter 4

Conclusions

Sustainable aviation fuel (SAF) is anticipated to be a viable near-future solution for aviation carbon emission reduction since non-drop-in fuels like hydrogen and electricity will take longer to develop and adopt. However, feedstocks in commercial production like residue and waste cannot meet the SAF demand in 2050 [9]. Energy crops as feedstock will be likely a crucial component for scaling up SAF production because of their high quantity. This study analyzes the global SAF production potential through crop allocation optimization.

This study has shown that there is substantial potential land that could be used for global SAF production. Under the GFDL-ESM2M climate model, using suitable land excluding cropland, forest, and protected land can meet the land requirement for biomass cultivation for the aviation sector, which requires 1.27% to 1.34% of expansion land use in 2050. With the expansion of potential land, the biomass yield surpasses the agricultural yield cultivated solely in cropland.

Under baseline assumptions in this analysis when 9 energy crops are selected as feedstocks for four scenario-year pairs and carbon intensity (CI) values of SAF pathways are set as the summation of core LCA and ILUC, the U.S. jet fuel demand can be met with 21.3% emissions saving when the objective is to minimize emissions while meeting demand under Scenario 1 (S1) in 2050. It is possible to produce 11.7% more SAF when optimizing for maximum fuel

production. 74.2% of suitable and available land is used even when optimized for minimum land use. Sorghum is the crop that contributes to SAF production the most in MinL and MaxF objectives, but the largest contributor is rapeseed for MinE. Additionally, by adding sugarbeet (SIP pathway) into SAF production, the maximum SAF production increases by 38.4% of 2050 U.S. jet fuel demand, and the emission is reduced by 42.4% and 47.7% of the emission threshold associated with petroleum jet fuel for MinE and MinL respectively, and only 40.6% of suitable land is needed for cultivation. However, the contribution of SAF production from sugarbeet exceeds the maximum blend ratio of 10% for its associated pathway, making it unrealistic. The results also highlight the potential of switchgrass and miscanthus (lignocellulosic biomass) as feedstocks. With switchgrass and miscanthus, the maximum SAF production is similar to the assumption with sugarbeet but with an additional 50% emission saving.

The analysis also demonstrates that SAF potential varies across countries, which is quantified with a linearized SAF potential showing that some countries cannot meet their own demand whereas others can far exceed it. Japan and the United Kingdom have an SAF production deficit since the jet fuel demand cannot be fulfilled with SAF in the near future. The U.S. can just meet demand in 2050, but not in 2100 given the land use limitation. Australia, Kenya, and Brazil have the SAF production surpluses in both 2050 and 2100 under a range of scenarios.

Furthermore, the land type converted to cropland for feedstock cultivation varies among countries based on the factors that limit SAF production. The strategy for land conversion doesn't change much for different objective functions if the suitable land area restricts the SAF production. Instead, when the emission threshold constrains the SAF production, the land conversion strategy will modified according to emission intensity (tCO_2e/ha) and fuel production efficiency (SAF MJ/ha) of different land types.

Future work could consider including more scenarios of interest such as SSP5 with RCP8.5, the highest emission scenario, which was not included in this study due to lack

of data on pastureland availability. Additionally, considering double cropping would be a valuable study to evaluate the potential to increase SAF production even more. Furthermore, the supply chain cost optimization could be included to better compare pathways with feedstocks other than energy crops. Finally, the framework developed in this analysis can expand to analyze the co-products of each pathway to evaluate the bio-energy potential.

Appendix A

Model Input Values

Table A.1: Conversion factors of Feedstock from GAEZ unit to SAF for ATJ pathway.

Crop	**GAEZ Unit**	$f_{GtIl}\left(\frac{kg_G}{kg_{WW}}\right)$	$f_{ItE}\left(\frac{kg_{WW}}{MJ_{EtOH}}\right)$	$f_{EtJl}\left(\frac{MJ_{EtOH}}{MJ_{Jet}}\right)$	**Source**
Maize	kg DW	0.845	0.111	1.78	[5, 16, 40]
Sugarcane	kg Sugar	0.12	0.586	1.78	[5, 39]
Sorghum	kg DW	0.876	0.113	1.78	[5, 32]
Crop	**GAEZ Unit**	$f_{GtIl}\left(\frac{kg_G}{kg_{DW}}\right)$	$f_{ItE}\left(\frac{kg_{DW}}{MJ_{EtOH}}\right)$	$f_{EtJl}\left(\frac{MJ_{EtOH}}{MJ_{Jet}}\right)$	**Source**
Wheat	kg DW	–	0.157	1.78	[11, 33]

Table A.2: Conversion factors of Miscanthus and Switchgrass from GAEZ unit to SAF for FT pathway [5, 48].

Crop	**GAEZ Unit**	$f_{GtIl}\left(\frac{kg_G}{kg_{DW}}\right)$	$f_{ItE}\left(\frac{kg_{DW}}{MJ_{Jet}}\right)$
Miscanthus	10 kg DW	0.1	0.240
Swichgrass	10 kg DW	0.1	0.255

Table A.3: Conversion factors of Feedstock from GAEZ unit to SAF for HEFA pathway.

Crop	**GAEZ Unit**	$f_{GtOl}\left(\frac{kg_G}{kg_{Oil}}\right)$	$f_{OtJ}\left(\frac{kg_{Oil}}{MJ_{Jet}}\right)$	**Source**
Soybean	kg DW	4.614	0.0295	[2, 24]
Rapeseed	kg DW	2.189	0.0295	[24, 30]
Sunflower	kg DW	2.17	0.0295	[24, 31]
Jatropha	kg DW	2.425	0.0289	[13, 24, 26]
Oil Palm	kg Oil	–	0.0289	[13, 24, 26]

Table A.4: Conversion factors of Feedstock from GAEZ unit to SAF for SIP pathway[14, 20].

Crop	**GAEZ Unit**	$f_{GtI}\left(\frac{kg_G}{kg_{kgDW}}\right)$	$f_{ItJ}\left(\frac{kg_{kgDW}}{MJ_{Jet}}\right)$
Sugar beet	kg Sugar	0.269	0.217

Table A.5: Projected U.S. Jet Fuel Demand [23].

Year	**Jet Fuel Demand (Billion Gallons)**
2019	18.96
2030	23.51
2050	31.79
2100	52.49

Table A.6: Life Cycle Assessment Values for each crop.

Crop	**Core LCA**	**ILUC**	**LCA**	**Source**
Jatropha	46.9	-24.8	22.1	[24]
Rapeseed	47.4	24.1	71.5	[24]
Sunflower	38.5	79	117.5	[24]
Sugarcane	24.1	8.5	32.6	[8, 24, 42]
Maize	55.8	29.7	85.5	[24]
Wheat	79.3	22	101.3	[6, 8, 24, 29]
Soybean	40.4	25.8	66.2	[24]
Oil Palm	37.4	39.1	76.5	[24]
Miscanthus	10.4	-12.6	-2.2	[24]
Swichgrass	10.4	5.3	15.7	[24]
Sugarbeet	32.4	11.2	43.6	[24]
Sorghum	78.2	20	98.2	[6, 8, 24, 29]

Appendix B

Additional Results

Table B.1: Pastureland land availability from 2030 to 2100 under S1 and S2.

	Pastureland Availability	
Year	**Scenario 1 (S1)**	**Scenario 2 (S2)**
2030	70%	64%
2040	68%	62%
2050	65%	60%
2060	63%	59%
2070	63%	58%
2080	64%	57%
2090	65%	57%
2100	67%	57%

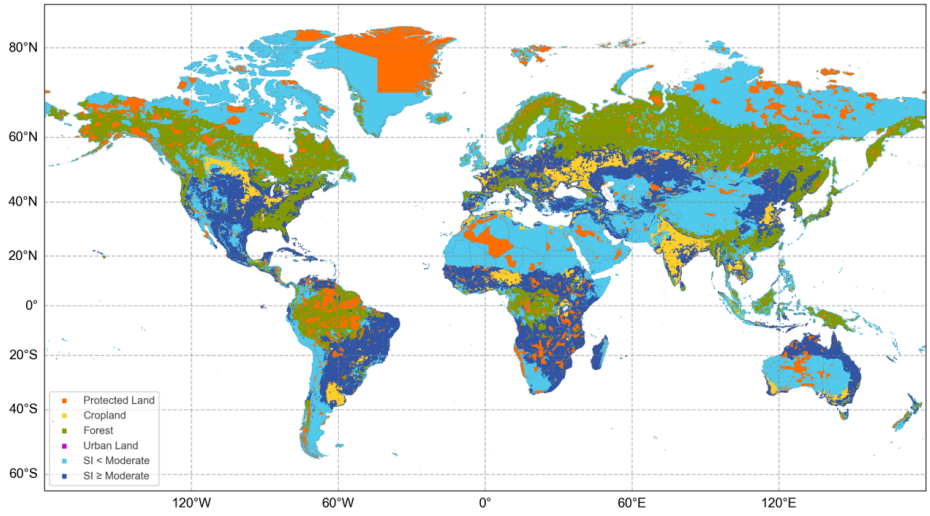

(a) S1, 2050

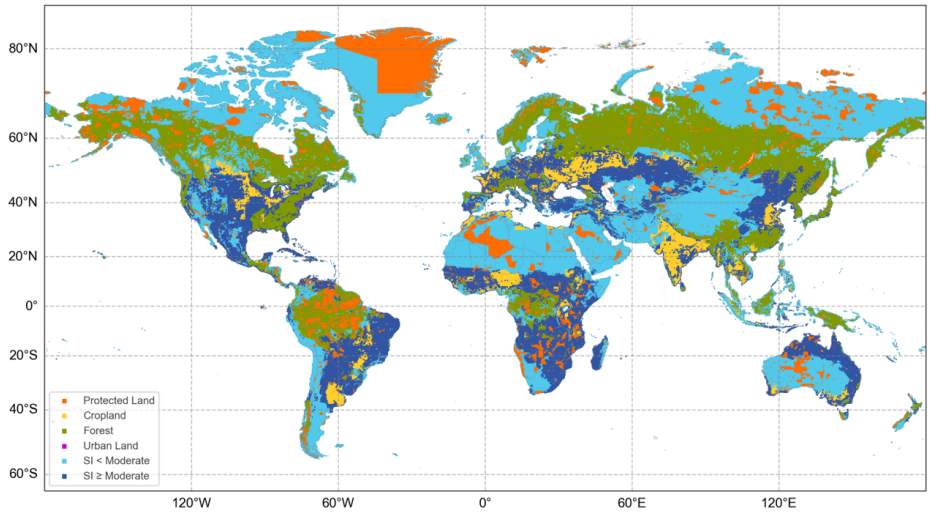

(b) S1, 2100

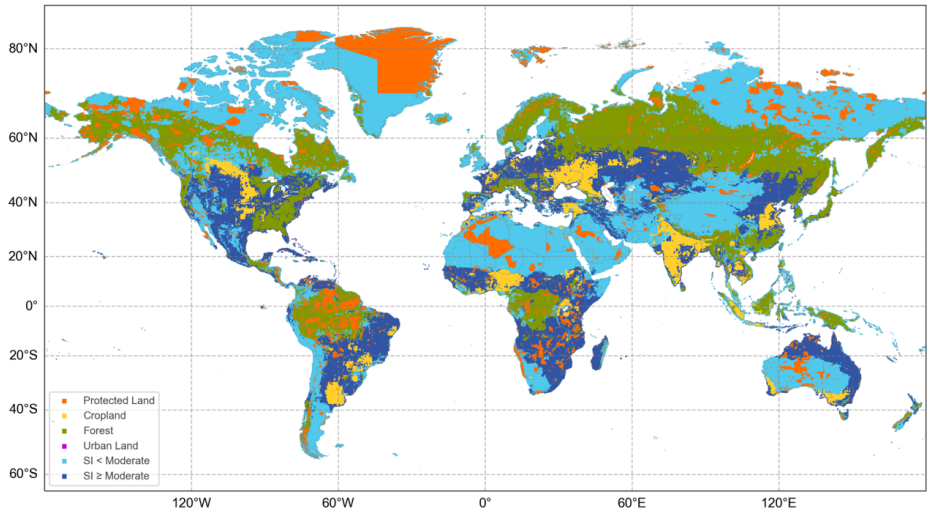

(c) S2, 2100

Figure B.1: Map of land use by category.

Table B.2: Projected agricultural yield of crops considered as feedstock for SAF production in the United States.

	Agricultural Yield [Million tonnes]			
Feedstock	**S1 2050**	**S1 2100**	**S2 2050**	**S2 2100**
Maize	1357.24	1339.14	1252.19	1188.80
Wheat	1385.66	1353.95	1306.26	1170.47
Sorghum	1320.11	1262.35	1162.99	1143.25
Sugarbeet	809.89	772.79	721.89	662.55
Soybean	584.24	599.87	559.98	494.19
Sunflower	551.93	548.47	520.47	458.83
Rapeseed	536.91	526.73	506.48	455.41
Sugarcane	187.78	229.55	217.41	205.25
Switchgrass	294.94	285.29	274.94	237.65
Miscanthus	192.66	199.64	185.10	170.23
Jatropha	85.86	96.27	94.67	88.85
Oil palm	2.79	3.53	2.77	4.20

Table B.3: SAF production and emission outputs optimized by three objectives for 2050 and 2100 in the U.S., data for Figure 3.4.

Objective	**Scenario**	**Year**	**SAF Production [Bgal]**	**Emission [Mt]**	**Land Usage [Mha]**
MinE	S1	2050	31.79	299.32	172.53
		2100	0.00	0.00	0.00
	S2	2050	0.00	0.00	0.00
		2100	0.00	0.00	0.00
MinL	S1	2050	31.79	378.91	129.39
		2100	0.00	0.00	0.00
	S2	2050	0.00	0.00	0.00
		2100	0.00	0.00	0.00
MaxF	S1	2050	35.51	380.21	173.59
		2100	32.92	406.74	163.82
	S2	2050	28.81	347.94	147.00
		2100	25.62	295.12	138.10

Table B.4: SAF production (in billion gallons) by crop optimized by MinE, MinL, and MaxF for 2050 under S1 in the U.S., data for Figure 3.5.

	SAF Production [Bgal]		
Crop	**MinE**	**MinL**	**MaxF**
Jatropha	2.504	1.013	2.022
Maize	2.803	4.261	5.254
Oil Palm	0.000	0.421	0.272
Rapeseed	16.179	4.261	9.060
Sorghum	6.157	10.652	12.857
Sugarcane	3.556	3.200	3.506
Sunflower	0.006	8.147	2.024
Wheat	0.444	0.007	0.517
Soybean	0.144	0.000	0.000
Total	31.792	31.792	35.512

Table B.5: SAF production and emission outputs optimized by three objectives with sugarbeet for 2050 and 2100 in the U.S., data for Figure 3.7.

Objective	**Scenario**	**Year**	**SAF Production [Bgal]**	**Emission [Mt]**	**Land Usage [Mha]**
MinE	S1	2050	31.79	172.45	74.23
		2100	0.00	0.00	0.00
	S2	2050	31.79	191.84	100.42
		2100	0.00	0.00	0.00
MinL	S1	2050	31.79	200.63	70.76
		2100	0.00	0.00	0.00
	S2	2050	31.79	241.87	93.53
		2100	0.00	0.00	0.00
MaxF	S1	2050	49.14	380.21	169.93
		2100	43.60	355.60	160.15
	S2	2050	37.94	309.54	143.99
		2100	32.42	273.58	134.86

Table B.6: SAF production and emission outputs optimized by three objectives with switchgrass and miscanthus for 2050 and 2100 in the U.S., data for Figure 3.11.

Objective	Scenario	Year	SAF Production [Bgal]	Emission [Mt]	Land Usage [Mha]
MinE	S1	2050	31.79	44.50	65.65
		2100	0.00	0.00	0.00
	S2	2050	31.79	120.19	118.40
		2100	0.00	0.00	0.00
MinL	S1	2050	31.79	113.07	65.37
		2100	0.00	0.00	0.00
	S2	2050	31.79	186.16	99.26
		2100	0.00	0.00	0.00
MaxF	S1	2050	48.62	289.95	173.91
		2100	43.34	250.82	164.12
	S2	2050	37.31	236.33	147.38
		2100	31.18	226.60	138.19

Table B.7: Baseline SAF production and land usage by land type for all objectives under S1 2050 in the U.S., data for Figure 3.9.

Objective	Land Type	SAF Production [Bgal]	Land Usage [Mha]
MinE	Non-forested Primary	7.76	49.81
	Non-forested Secondary	6.99	30.98
	Pastureland	17.03	91.74
MinL	Non-forested Primary	7.44	32.49
	Non-forested Secondary	7.50	26.28
	Pastureland	16.86	70.62
MaxF	Non-forested Primary	8.48	50.38
	Non-forested Secondary	7.70	31.09
	Pastureland	19.34	92.13

Table B.8: Baseline SAF production and land usage by land type for all objectives under S1 2050 in Kenya, data for Figure 3.10.

Objective	Land Type	SAF Production [Bgal]	Land Usage [Mha]
MinE	Non-forested Primary	0.016	0.076
	Non-forested Secondary	0.14	0.78
	Pastureland	0.14	0.70
MinL	Non-forested Primary	0.041	0.12
	Non-forested Secondary	0.17	0.49
	Pastureland	0.081	0.21
MaxF	Non-forested Primary	0.058	0.31
	Non-forested Secondary	0.44	2.60
	Pastureland	0.44	2.33

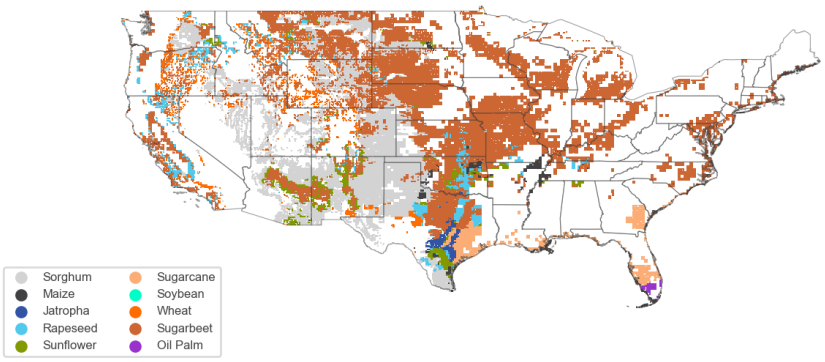

(a) MaxF

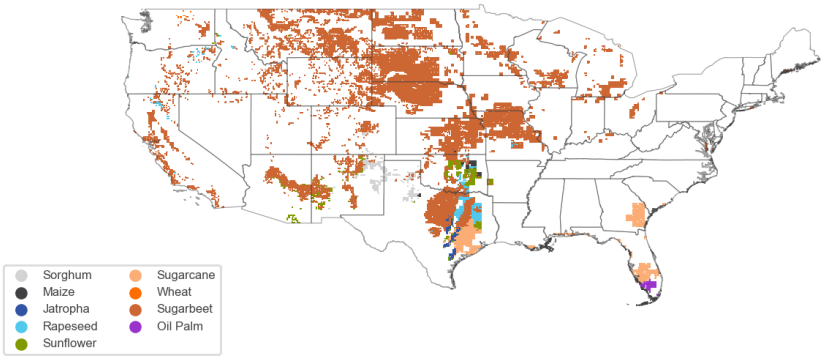

(b) MinL

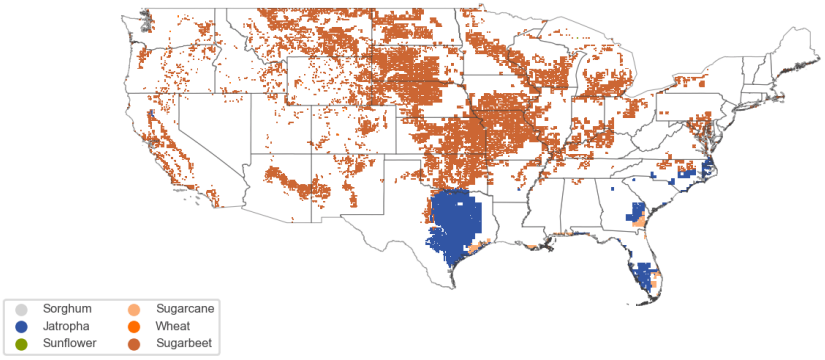

(c) MinE

Figure B.2: SAF production potential optimized with sugarbeet for MaxF (a), MinL (b), and MinE (c) for S1 2050.

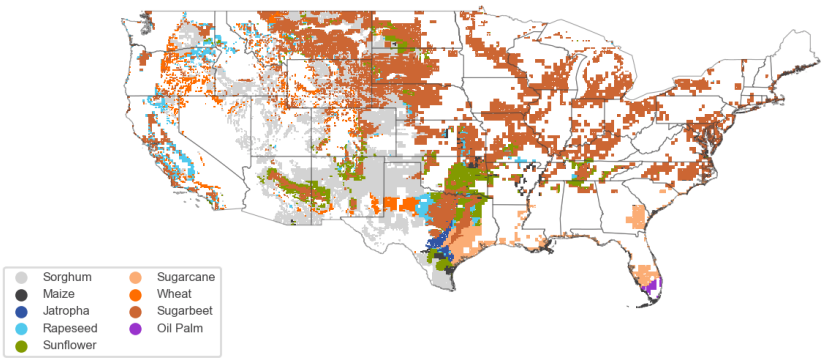

(a) MaxF

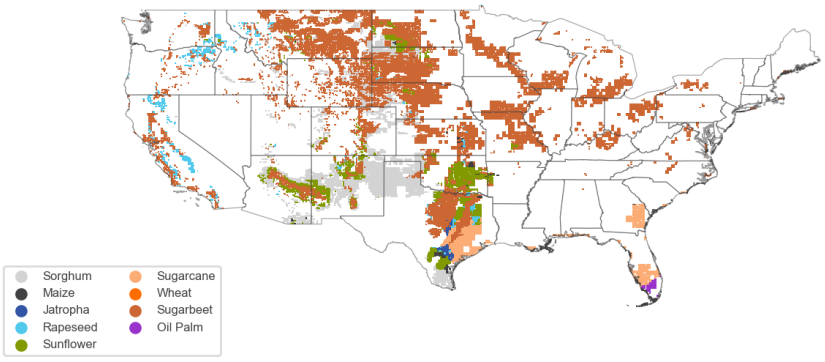

(b) MinL

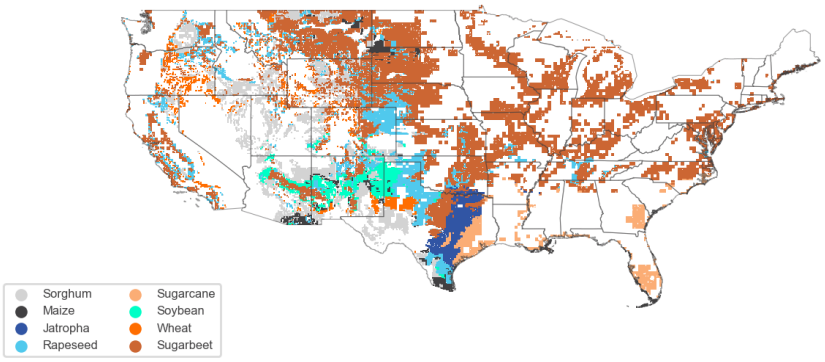

(c) MinE

Figure B.3: SAF production potential optimized with sugarbeet for MaxF (a), MinL (b), and MinE (c) for S2 2050.

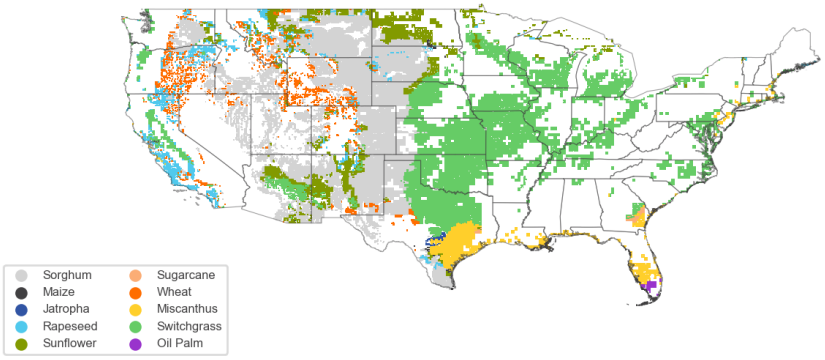

(a) MaxF

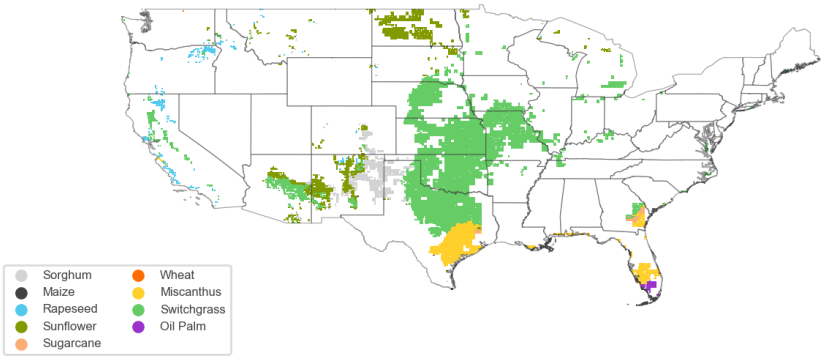

(b) MinL

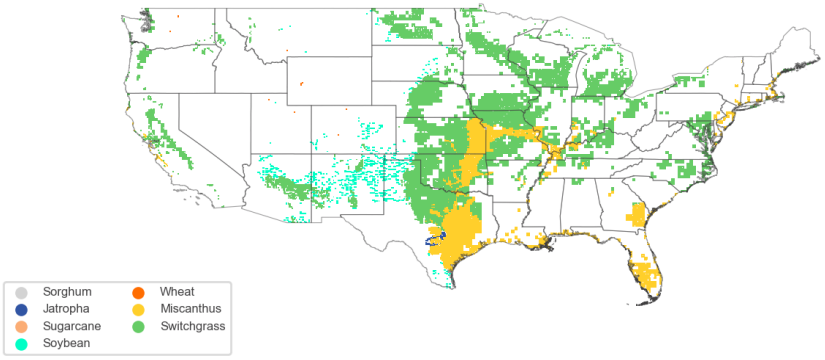

(c) MinE

Figure B.4: SAF production potential optimized with switchgrass and miscanthus for MaxF (a), MinL (b), and MinE (c) for S1 2050.

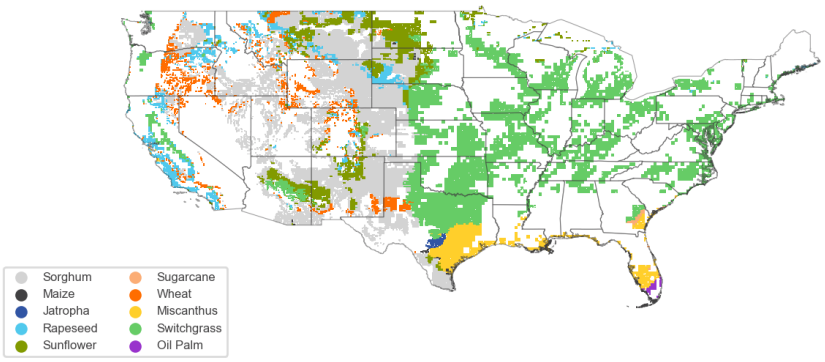

(a) MaxF

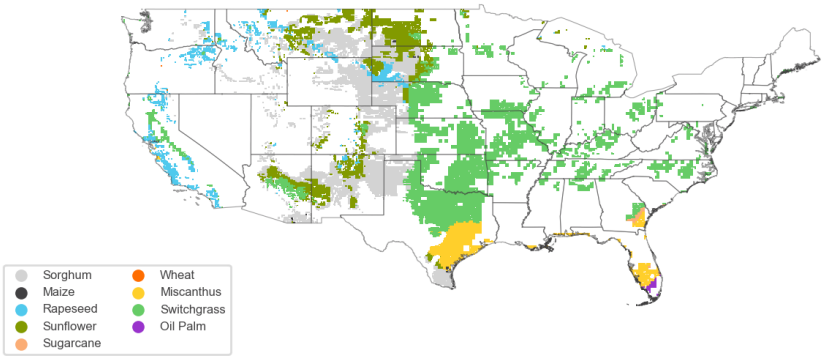

(b) MinL

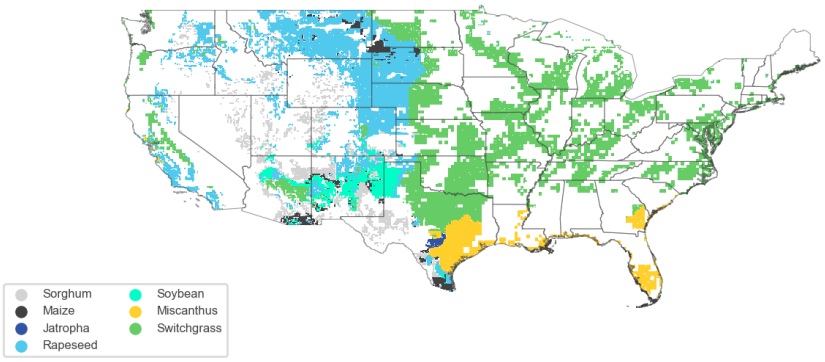

(c) MinE

Figure B.5: SAF production potential optimized with switchgrass and miscanthus for MaxF (a), MinL (b), and MinE (c) for S2 2050.

Appendix C

Results - Kenya

Table C.1: SAF production, emission, and land use outputs for 2050 and 2100 in Kenya.

Objective	**Scenario**	**Year**	**SAF Production [Bgal]**	**Emission [Mt]**	**Land Usage [Mha]**
MinE	S1	2050	0.30	0.88	1.55
		2100	0.49	1.45	2.60
	S2	2050	0.30	0.88	1.53
		2100	0.49	1.45	2.56
MinL	S1	2050	0.30	3.53	0.82
		2100	0.49	5.83	1.53
	S2	2050	0.30	3.04	0.79
		2100	0.49	5.55	1.26
MaxF	S1	2050	0.94	3.53	5.24
		2100	1.22	5.83	8.14
	S2	2050	0.86	3.53	4.74
		2100	1.20	5.83	7.66

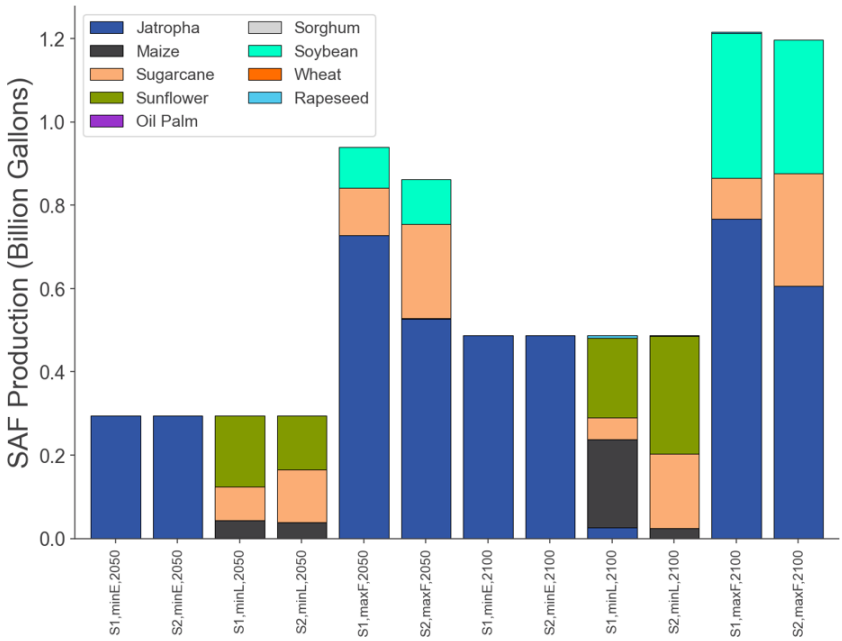

Figure C.1: SAF production by crop optimized for all objectives under S1 and S1 in 2050 and 2100 in Kenya.

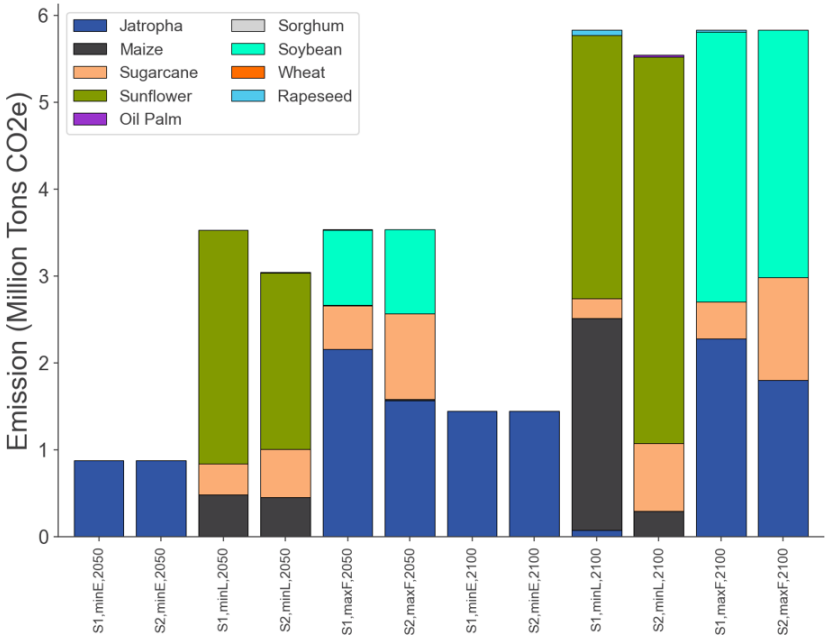

Figure C.2: Emission by crop optimized for all objectives under S1 and S1 in 2050 and 2100 in Kenya.

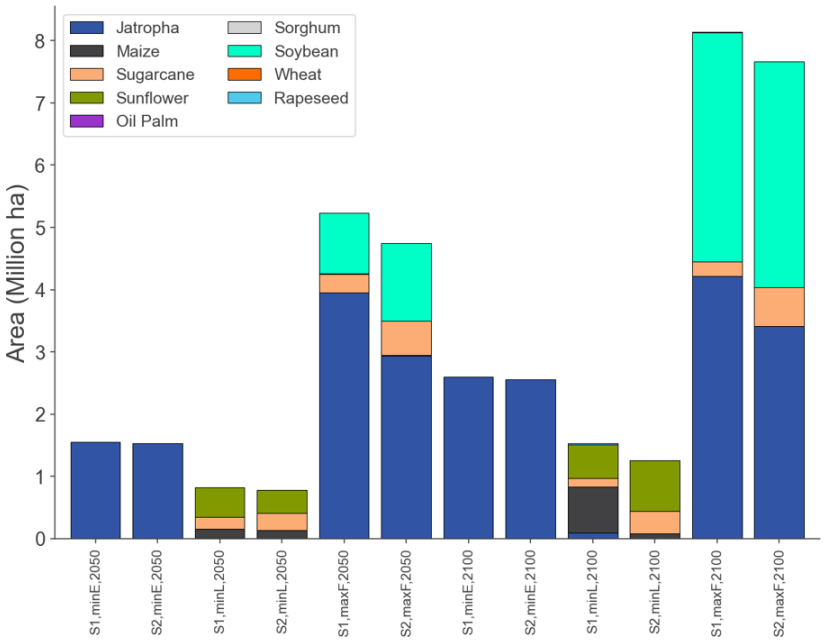

Figure C.3: Land area by crop optimized for all objectives under S1 and S1 in 2050 and 2100 in Kenya.

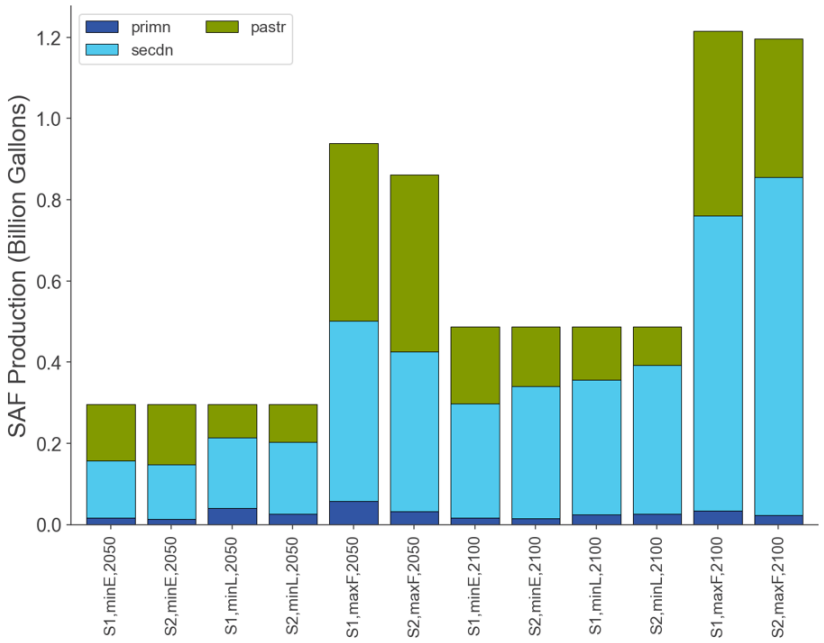

Figure C.4: SAF production by land optimized for all objectives under S1 and S1 in 2050 and 2100 in Kenya.

Appendix D

Results - Japan

Table D.1: SAF production, emission, and land use outputs optimized for 2050 and 2100 in Japan.

Objective	**Scenario**	**Year**	**SAF Production [Bgal]**	**Emission [Mt]**	**Land Usage [Mha]**
MaxF	S1	2050	0.15	1.71	0.60
		2100	0.16	1.72	0.62
	S2	2050	0.14	1.35	0.56
		2100	0.15	1.53	0.58

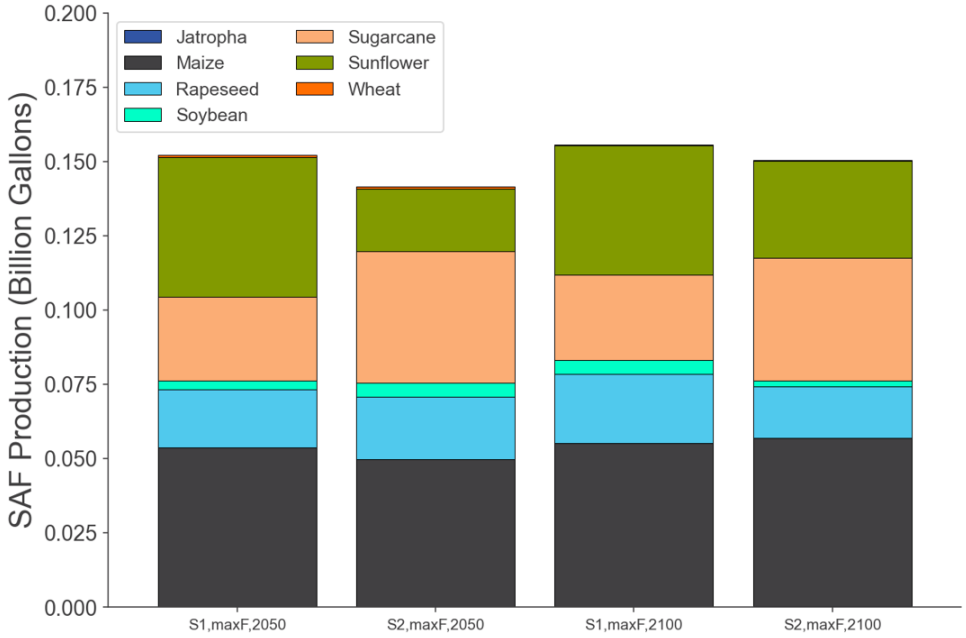

Figure D.1: SAF production by crop under S1 and S1 in 2050 and 2100 in Japan.

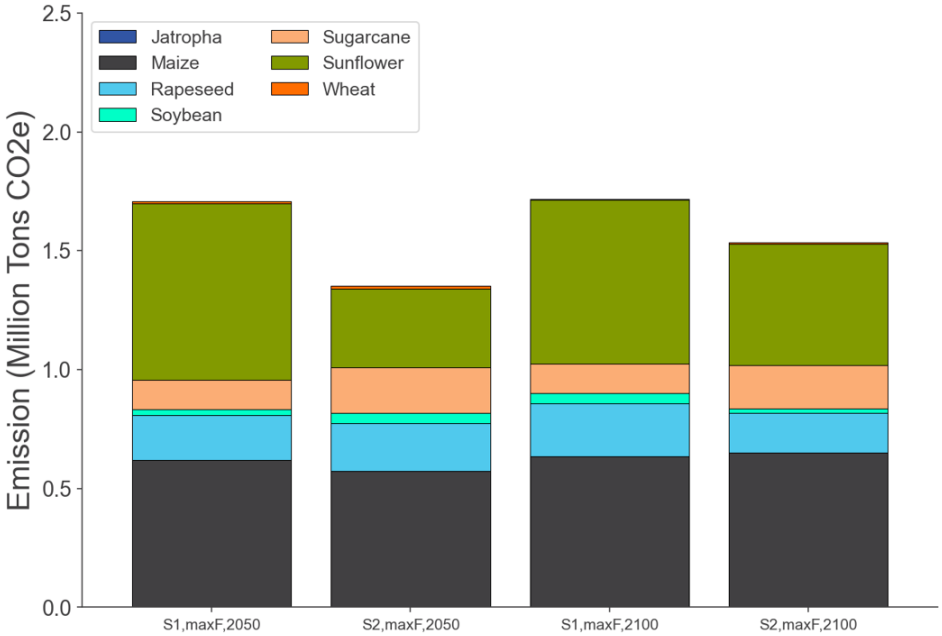

Figure D.2: Emission by crop under S1 and S1 in 2050 and 2100 in Japan.

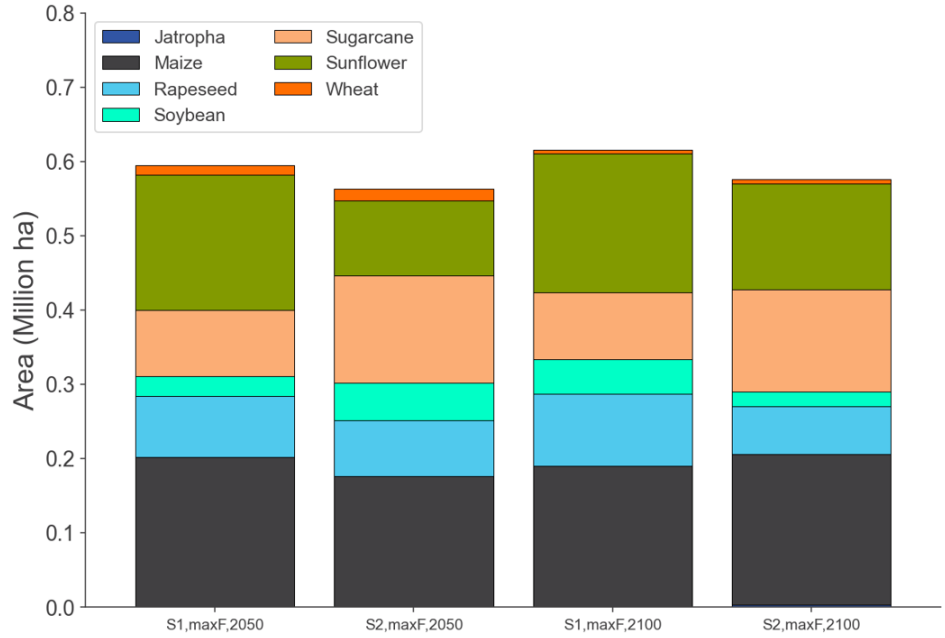

Figure D.3: Land area by crop under S1 and S1 in 2050 and 2100 in Japan.

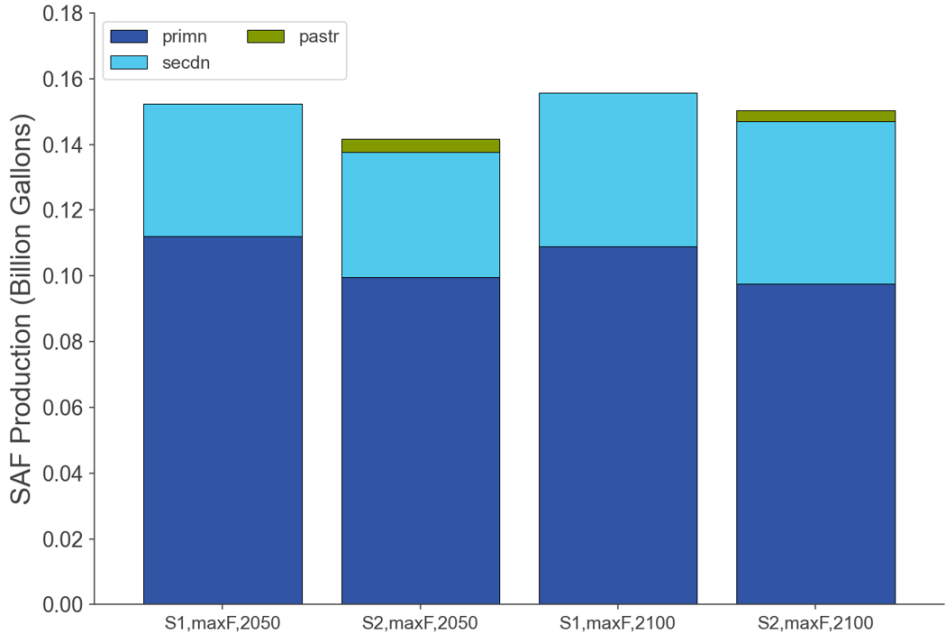

Figure D.4: SAF production by land under S1 and S1 in 2050 and 2100 in Japan.

Appendix E

Results - United Kingdom

Table E.1: SAF production, emission, and land use outputs optimized for 2050 and 2100 in the United Kingdom.

Objective	**Scenario**	**Year**	**SAF Production [Bgal]**	**Emission [Mt]**	**Land Usage [Mha]**
MaxF	S1	2050	0.86	8.22	3.49
		2100	0.76	7.33	3.17
	S2	2050	0.65	6.20	2.67
		2100	1.04	9.97	3.84

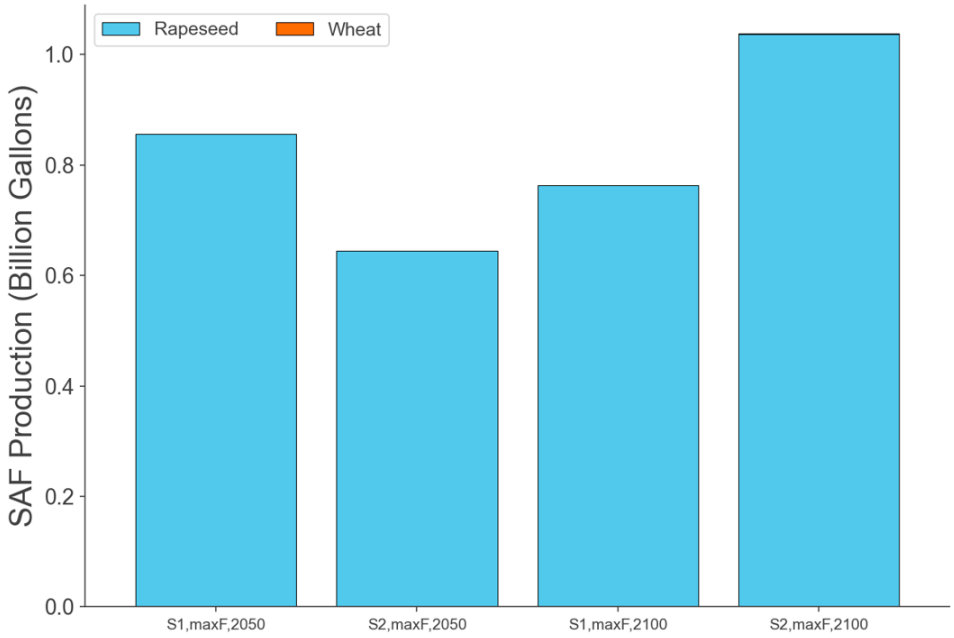

Figure E.1: SAF production by crop under S1 and S1 in 2050 and 2100 in the United Kingdom.

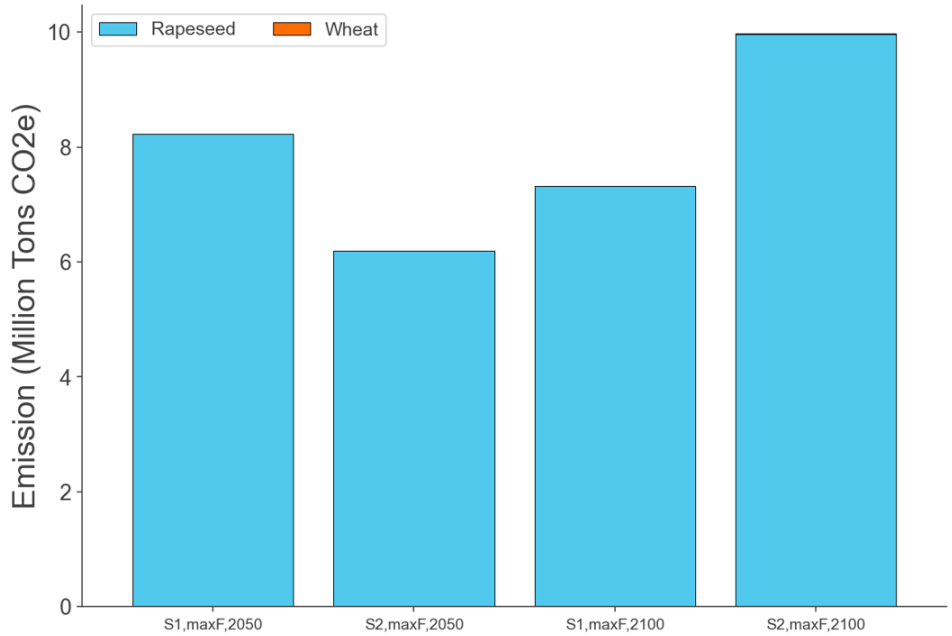

Figure E.2: Emission by crop under S1 and S1 in 2050 and 2100 in the United Kingdom.

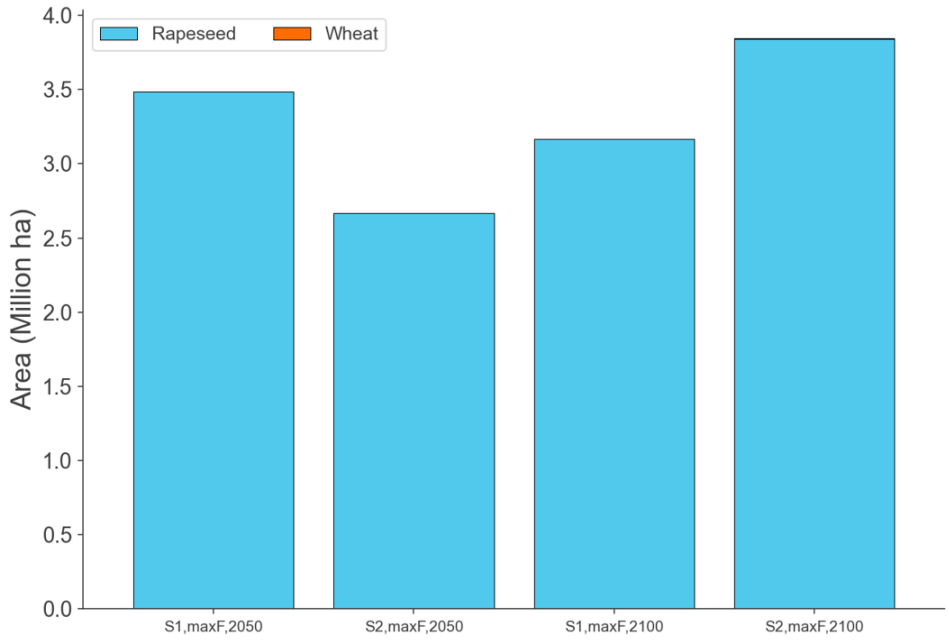

Figure E.3: Land area by crop under S1 and S1 in 2050 and 2100 in the United Kingdom.

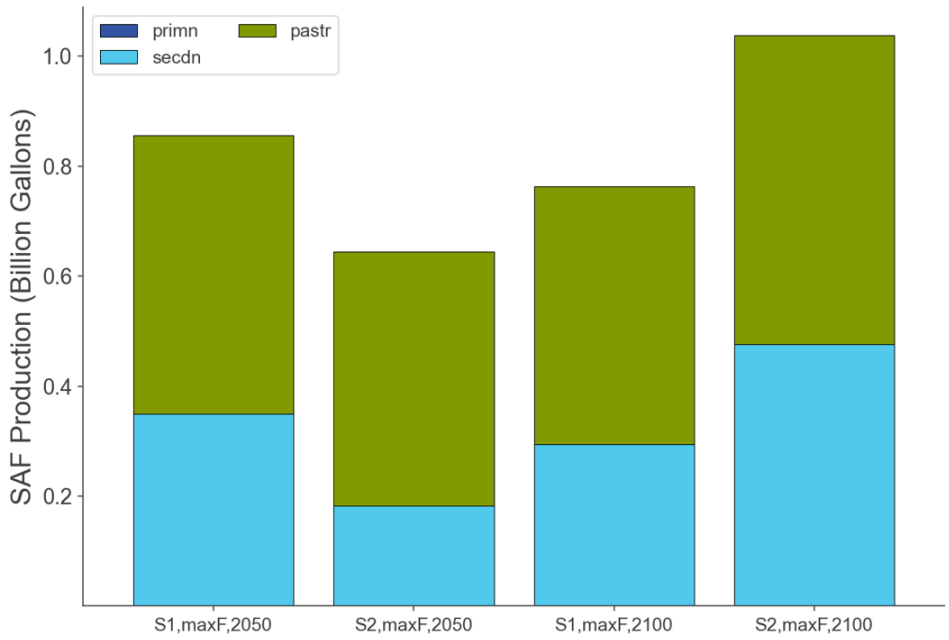

Figure E.4: SAF production by land under S1 and S1 in 2050 and 2100 in the United Kingdom.

Appendix F

Results - Australia

Table F.1: SAF production, emission, and land use outputs for 2050 and 2100 in Australia.

Objective	**Scenario**	**Year**	**SAF Production [Bgal]**	**Emission [Mt]**	**Land Usage [Mha]**
MinE	S1	2050	3.64	26.79	32.06
		2100	6.01	45.57	56.46
	S2	2050	3.64	26.16	31.49
		2100	6.01	43.97	54.74
MinL	S1	2050	3.64	43.47	11.67
		2100	6.01	70.74	19.83
	S2	2050	3.64	43.17	12.36
		2100	6.01	70.02	19.13
MaxF	S1	2050	5.52	43.53	54.90
		2100	8.91	71.87	87.55
	S2	2050	5.60	43.53	54.08
		2100	9.11	71.87	100.00

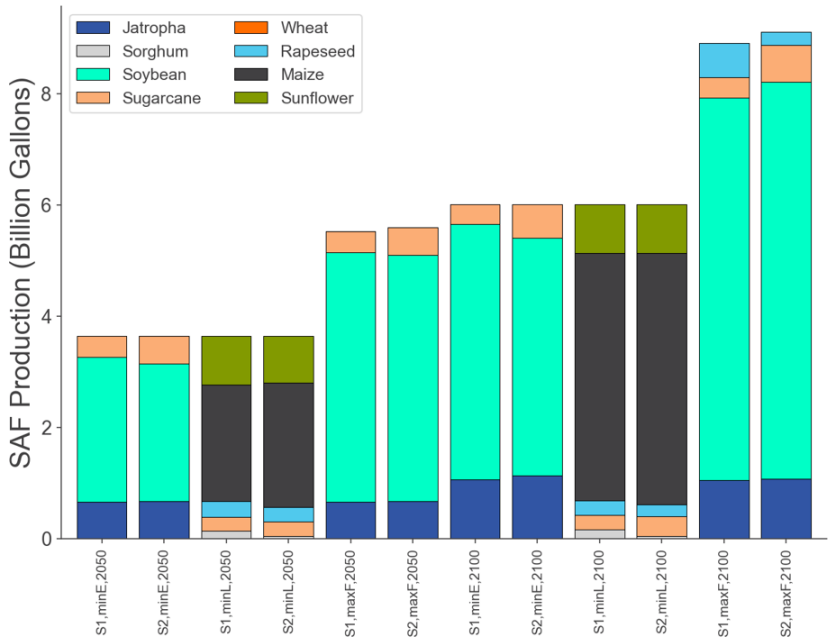

Figure F.1: SAF production by crop optimized for all objectives under S1 and S1 in 2050 and 2100 in Australia.

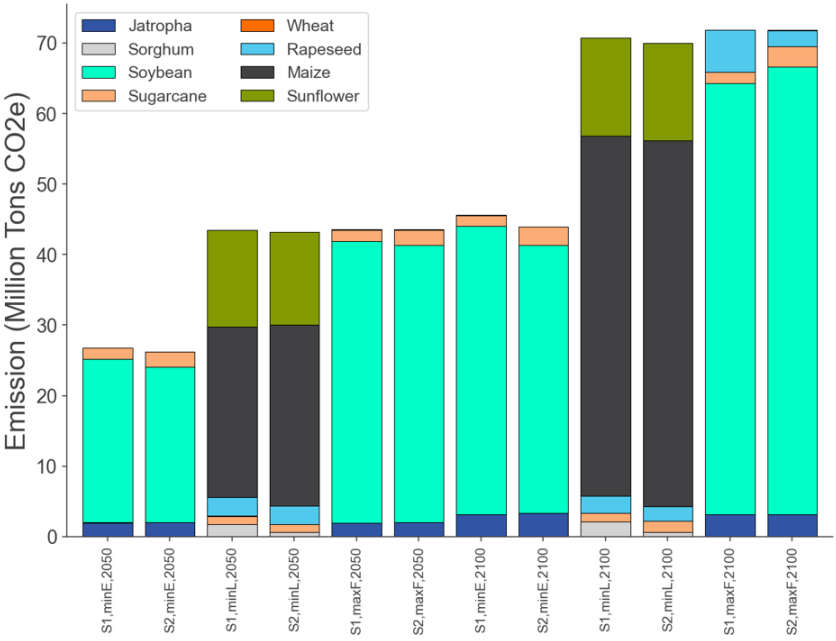

Figure F.2: Emission by crop optimized for all objectives under S1 and S1 in 2050 and 2100 in Australia.

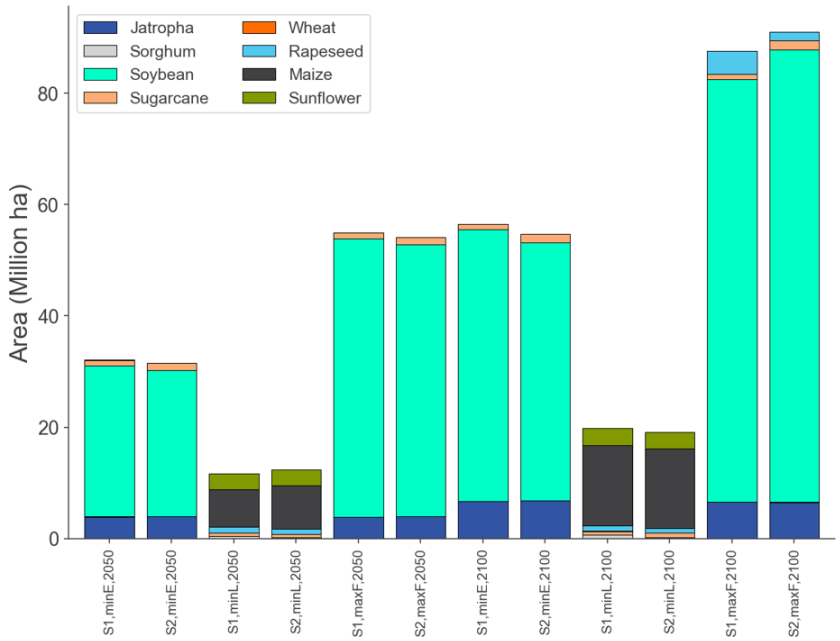

Figure F.3: Land area by crop optimized for all objectives under S1 and S1 in 2050 and 2100 in Australia.

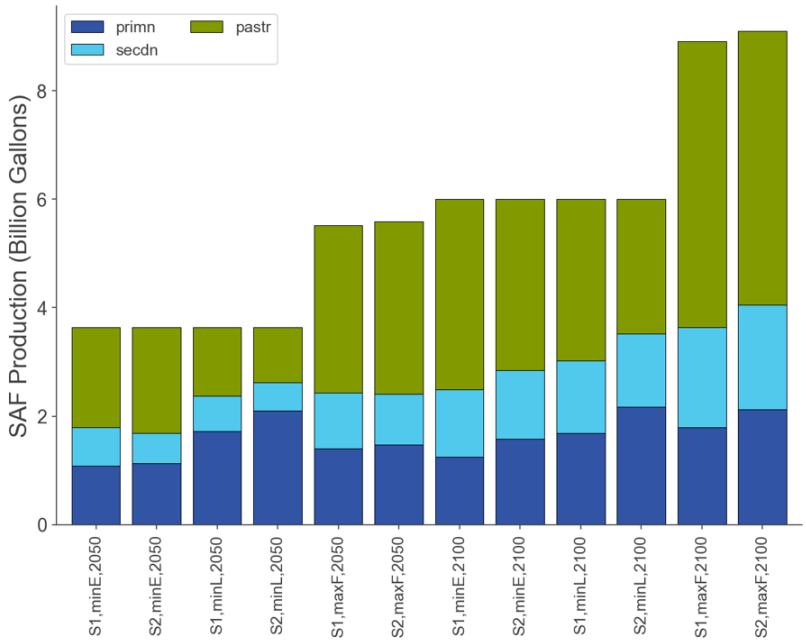

Figure F.4: SAF production by land optimized for all objectives under S1 and S1 in 2050 and 2100 in Australia.

Appendix G

Results - Brazil

Table G.1: SAF production, emission, and land use outputs for 2050 and 2100 in Brazil.

Objective	**Scenario**	**Year**	**SAF Production [Bgal]**	**Emission [Mt]**	**Land Usage [Mha]**
MinE	S1	2050	2.59	7.69	11.99
		2100	4.28	12.70	21.61
	S2	2050	2.59	7.69	14.29
		2100	4.28	12.70	24.02
MinL	S1	2050	2.59	23.22	4.40
		2100	4.28	43.44	6.60
	S2	2050	2.59	25.29	5.32
		2100	4.28	46.88	9.83
MaxF	S1	2050	10.43	30.99	54.89
		2100	17.23	51.16	92.77
	S2	2050	10.43	30.99	58.78
		2100	15.23	51.16	75.74

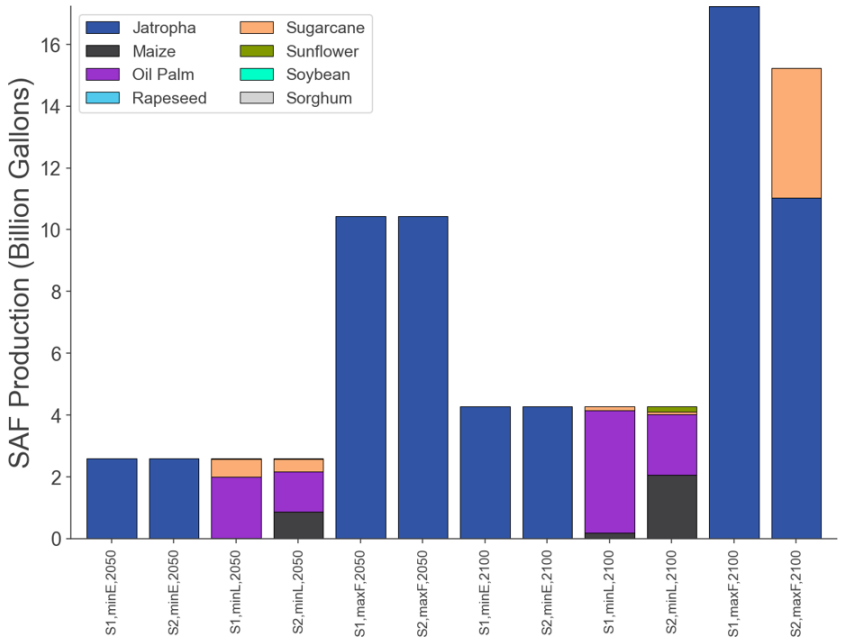

Figure G.1: SAF production by crop optimized for all objectives under S1 and S1 in 2050 and 2100 in Brazil.

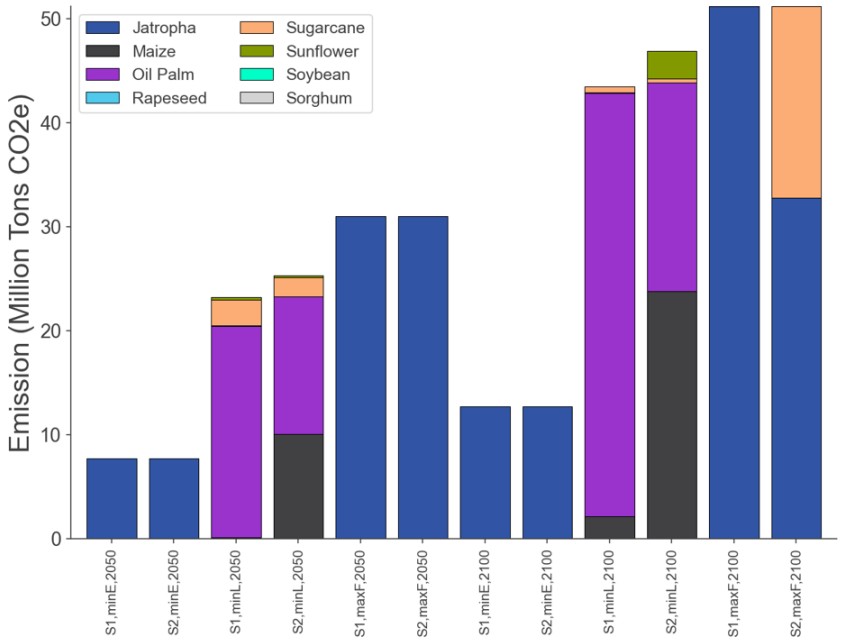

Figure G.2: Emission by crop optimized for all objectives under S1 and S1 in 2050 and 2100 in Brazil.

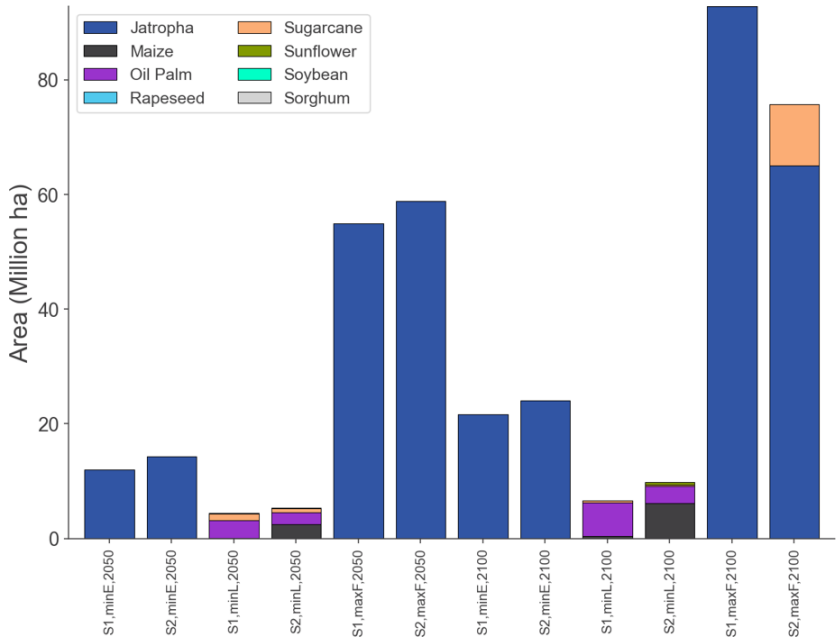

Figure G.3: Land area by crop optimized for all objectives under S1 and S1 in 2050 and 2100 in Brazil.

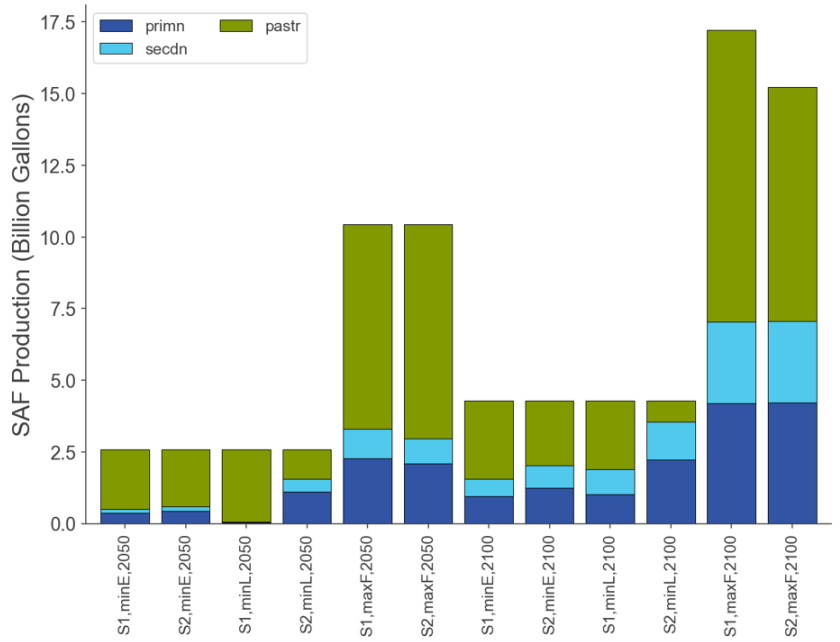

Figure G.4: SAF production by land optimized for all objectives under S1 and S1 in 2050 and 2100 in Brazil.

References

[1] (2015). Coastadapt infographics. National Climate Change Adaptation Research Facility. Available online: https://coastadapt.com.au/sites/default/files/infographics/15-117-NCCARFINFOGRAPHICS-01-UPLOADED-WEB%2827Feb%29.pdf.

[2] (n.d.). Conversion table. https://ussec.org/resources/conversion-table/. Last accessed February 6, 2024.

[3] Airbus (2023). Global market forecast. https://www.airbus.com/en/products-services/commercial-aircraft/market/global-market-forecast. Accessed: 2024-03-06.

[4] American Society for Testing and Materials (2022). Astm d7566-22, standard specification for aviation turbine fuel containing synthesized hydrocarbons. https://www.astm.org/DATABASE.CART/HISTORICAL/D7566-22.htm.

[5] Argonne National Laboratory (2022). Greenhouse gases, regulated emissions, and energy use in technologies (greet) model. Accessed: 2024-01-21.

[6] Cai, H., Dunn, J. B., Wang, Z., Han, J., and Wang, M. Q. (2013). Life-cycle energy use and greenhouse gas emissions of production of bioethanol from sorghum in the united states. *Biotechnology for Biofuels*, 6(1):141.

[7] Cantarella, H., Nassar, A. M., Cortez, L. A. B., and Baldassin, R. (2015). Potential feedstock for renewable aviation fuel in brazil. *Environmental Development*, 15:52–63.

[8] Cerulogy (2019). Risk management for biofuel policies in the context of uncertain emission savings. Cerulogy Report. Accessed: 2024-02-19.

[9] Chung, Jacob (2013). Grand challenges in bioenergy and biofuel research: Engineering and technology development, environmental impact, and sustainability. *Frontiers in Energy Research*, 1.

[10] Core Writing Team, Pachauri, R., and Meyer, L. (2014). *Climate Change 2014: Synthesis Report. Contribution of Working Groups I, II and III to the Fifth Assessment Report of the Intergovernmental Panel on Climate Change*. Geneva, Switzerland.

[11] Demsky, S. E. (2023). Analysis of double cropping to expand sustainable aviation fuel production in the united states.

[12] FAO and IIASA (2024). Global agro ecological zones version 4 (gaez v4). [Online]. 2024.01.20.

[13] Grimsby, L. K., Aune, J. B., and Johnsen, F. H. (2012). Human energy requirements in jatropha oil production for rural electrification in tanzania. *Energy for Sustainable Development*, 16(3):297–302.

[14] Gruska, R. M., Baryga, A., Kunicka-Styczynska, A., Brzezinski, S., Rosicka-Kaczmarek, J., Miskiewicz, K., and Suminska, T. (2022a). Fresh and stored sugar beet roots as a source of various types of mono- and oligosaccharides. *Molecules*, 27(16):5125.

[15] Gruska, R. M., Baryga, A., Kunicka-Styczzyńska, A., Brzeziński, S., Rosicka-Kaczmarek, J., Miśkiewicz, K., and Sumińska, T. (2022b). Fresh and stored sugar beet roots as a source of various types of mono- and oligosaccharides. https://doi.org/10.3390/molecules27165125.

[16] Hicks, D. R. and Cloud, H. A. (1991). *Calculating Grain Weight Shrinkage in Corn Due to Mechanical Drying*. National Corn Handbook. URL accessed Dec 2021.

[17] Hurtt, G. C., Chini, L., Sahajpal, R., Frolking, S., Bodirsky, B. L., Calvin, K., Doelman, J., Fisk, J., Fujimori, S., Goldewijk, K. K., Hasegawa, T., Havlik, P., Heinimann, A., Humpenöder, F., Jungclaus, J., Kaplan, J., Krisztin, T., Lawrence, D., Lawrence, P., Mertz, O., Pongratz, J., Popp, A., Riahi, K., Shevliakova, E., Stehfest, E., Thornton, P., van Vuuren, D., and Zhang, X. (2019a). Harmonization of global land use change and management for the period 2015-2300. version 20190529.

[18] Hurtt, G. C., Chini, L., Sahajpal, R., Frolking, S., Bodirsky, B. L., Calvin, K., Doelman, J., Fisk, J., Fujimori, S., Goldewijk, K. K., Hasegawa, T., Havlik, P., Heinimann, A., Humpenöder, F., Jungclaus, J., Kaplan, J., Krisztin, T., Lawrence, D., Lawrence, P., Mertz, O., Pongratz, J., Popp, A., Riahi, K., Shevliakova, E., Stehfest, E., Thornton, P., van Vuuren, D., and Zhang, X. (2019b). Harmonization of global land use change and management for the period 850-2015. version 20190529.

[19] Hurtt, G. C., Chini, L., Sahajpal, R., Frolking, S., Bodirsky, B. L., Calvin, K., Doelman, J., Fisk, J., Fujimori, S., Goldewijk, K. K., Hasegawa, T., Havlik, P., Heinimann, A., Humpenöder, F., Jungclaus, J., Kaplan, J., Krisztin, T., Lawrence, D., Lawrence, P., Mertz, O., Pongratz, J., Popp, A., Riahi, K., Shevliakova, E., Stehfest, E., Thornton, P., van Vuuren, D., and Zhang, X. (2020). Harmonization of global land-use change and management for the period 850-2100 (luh2) for cmip6. *Geoscientifc Model Development Discussions*.

[20] Iii, K. and T, W. (2021). Cost optimization of us sustainable aviation fuel supply chain under different policy constraints.

[21] International Air Transport Association (2023a). Net zero 2050: sustainable aviation fuels. URL accessed March 4, 2024.

[22] International Air Transport Association (2023b). Saf deployment. URL accessed March 4, 2024.

[23] International Air Transport Association (2023c). Total fuel consumption of commercial airlines worldwide between 2005 and 2021, with a forecast until 2023 (in billion gallons) [graph]. Retrieved January 29, 2024.

[24] International Civil Aviation Organization (2023). Corsia supporting document: Corsia eligible fuels lca methodology. Accessed: 2024-01-21.

[25] International Energy Agency (IEA) (2023). Tracking clean energy progress 2023. https://www.iea.org/reports/tracking-clean-energy-progress-2023. Licence: CC BY 4.0.

[26] Jonas, M., Ketlogetswe, C., and Gandure, J. (2020). Variation of jatropha curcas seed oil content and fatty acid composition with fruit maturity stage. *Heliyon*, 6(1):e03285.

[27] Kriegler, E., Bauer, N., Popp, A., Humpenöder, F., Leimbach, M., Strefler, J., Baumstark, L., Bodirsky, B. L., Hilaire, J., Klein, D., Mouratiadou, I., Weindl, I., Bertram, C., Dietrich, J.-P., Luderer, G., Pehl, M., Pietzcker, R., Piontek, F., Lotze-Campen, H., and Edenhofer, O. (2017). Fossil-fueled development (ssp5): An energy and resource intensive scenario for the 21st century. *Global Environmental Change*, 42:297–315.

[28] Kucharska, K., Słupek, E., Cieśliński, H., and Kamiński, M. (2020). Advantageous conditions of saccharification of lignocellulosic biomass for biofuels generation via fermentation processes. *Chemical Papers*, 74(4):1199–1209.

[29] Lantz, M., Prade, T., Ahlgren, S., and Björnsson, L. (2018). Biogas and ethanol from wheat grain or straw: Is there a trade-off between climate impact, avoidance of iluc and production cost? *Energies*, 11(10).

[30] Mailer, R. (2016). Oilseeds: Overview. *Encyclopedia of Food Grains*.

[31] Matthaus, B., Özcan, M. M., and Al Juhaimi, F. (2016). Some rape/canola seed oils: fatty acid composition and tocopherols. *Zeitschrift fur Naturforschung. C, Journal of biosciences*, 71(3-4):73–77.

[32] McKenzie, B. and Richey, C. (2003). *Harvesting, Drying and Storing Grain Sorghum.* Purdue University Cooperative Extension Service. URL accessed Dec 2021.

[33] Neely, C. (2016). *Potential Income Losses in Harvesting Dry Wheat Grain.* Texas Row Crops Newsletter. Retrieved February 6, 2024.

[34] Ng, K. S., Farooq, D., and Yang, A. (2021). Global biorenewable development strategies for sustainable aviation fuel production. *Renewable and Sustainable Energy Reviews*, 150:111502.

[35] Riahi, K., van Vuuren, D. P., Kriegler, E., Edmonds, J., O'Neill, B. C., Fujimori, S., Bauer, N., Calvin, K., Dellink, R., Fricko, O., Lutz, W., Popp, A., Cuaresma, J. C., KC, S., Leimbach, M., Jiang, L., Kram, T., Rao, S., Emmerling, J., Ebi, K., Hasegawa, T., Havlík, P., Humpenöder, F., Silva, L. A. D., Smith, S., Stehfest, E., Bosetti, V., Eom, J., Gernaat, D., Masui, T., Rogelj, J., Strefler, J., Drouet, L., Krey, V., Luderer, G., Harmsen, M., Takahashi, K., Baumstark, L., Doelman, J. C., Kainuma, M., Klimont, Z., Marangoni, G., Lotze-Campen, H., Obersteiner, M., Tabeau, A., and Tavoni, M. (2017). The shared socioeconomic pathways and their energy, land use, and greenhouse gas emissions implications: An overview. *Global Environmental Change*, 42:153–168.

[36] Ritchie, H., Rosado, P., and Roser, M. (2019). Meat and dairy production.

[37] Rogelj, J. et al. (2016). Shared socioeconomic pathways (ssps). International Institute for Applied Systems Analysis (IIASA). Available online: https://unfccc.int/sites/default/files/part1_iiasa_rogelj_ssp_poster.pdf.

[38] Rondinelli, S., Gardi, A., Kapoor, R., and Sabatini, R. (2017). Benefits and challenges of liquid hydrogen fuels in commercial aviation. *International Journal of Sustainable Aviation*, 3(3):200–216.

[39] Sansoucy, R., Preston, T. R., and Leng, R. A., editors (1987). *Proceedings of the FAO Expert Consultation on the Substitution of Imported Concentrate Feeds in Animal*

Production Systems in Developing Countries, Bangkok. Food & Agriculture Org. Held in the FAO Regional Office for Asia and the Pacific, 9-13 September 1985.

[40] Santos, E., Mari, L., Reis, R., Ferreira, G., Brown, A., Bernardes, T., Ramos, E., Santos, W., de, O., Chavira, J., Refat, B., Yu, P., Unpaprom, Y., Ramaraj, R., and Hutňan, M. (2016). *Advances in Silage Production and Utilization*.

[41] Sarlioglu, B. and Morris, C. T. (2015). More electric aircraft: Review, challenges, and opportunities for commercial transport aircraft. *IEEE Transactions on Transportation Electrification*, 1(1):54–64.

[42] Schmidt, J. H. (2015). Life cycle assessment of five vegetable oils. *Journal of Cleaner Production*, 87:130–138.

[43] Staples, M. D., Malina, R., Suresh, P., Hileman, J. I., and Barrett, S. R. H. (2018). Aviation co2 emissions reductions from the use of alternative jet fuels. *Energy Policy*, 114:342–354.

[44] UNEP-WCMC and IUCN (2024). Protected planet: [protected areas (wdpa); the world database on protected areas (wdpa)/the world database on other effective area-based conservation measures (wd-oecm)/the global database on protected areas management effectiveness (gd-pame)]. [On-line]. Cambridge, UK: UNEP-WCMC and IUCN. Available at: www.protectedplanet.net.

[45] United States Census Bureau (2010). State area measurements and internal point co-ordinates. https://www.census.gov/geographies/reference-files/2010/geo/state-area.html. Accessed on March 12, 2024.

[46] United States Department of Agriculture (2024). Crop explorer country summary for major crop regions. Country Summary. Accessed: 2024-02-08.

[47] United States Geological Survey (2018). The water area of each state. United States Geological Survey. Retrieved January 29, 2024.

[48] Zang, G., Sun, P., Elgowainy, A., Bafana, A., and Wang, M. (2021). Life cycle analysis of electrofuels: Fischer–tropsch fuel production from hydrogen and corn ethanol byproduct co2. *Environmental Science & Technology*, 55(6):3888–3897.